LISTENING TO METEORS

Infrasonic Observations of Meteors in Northern Sweden

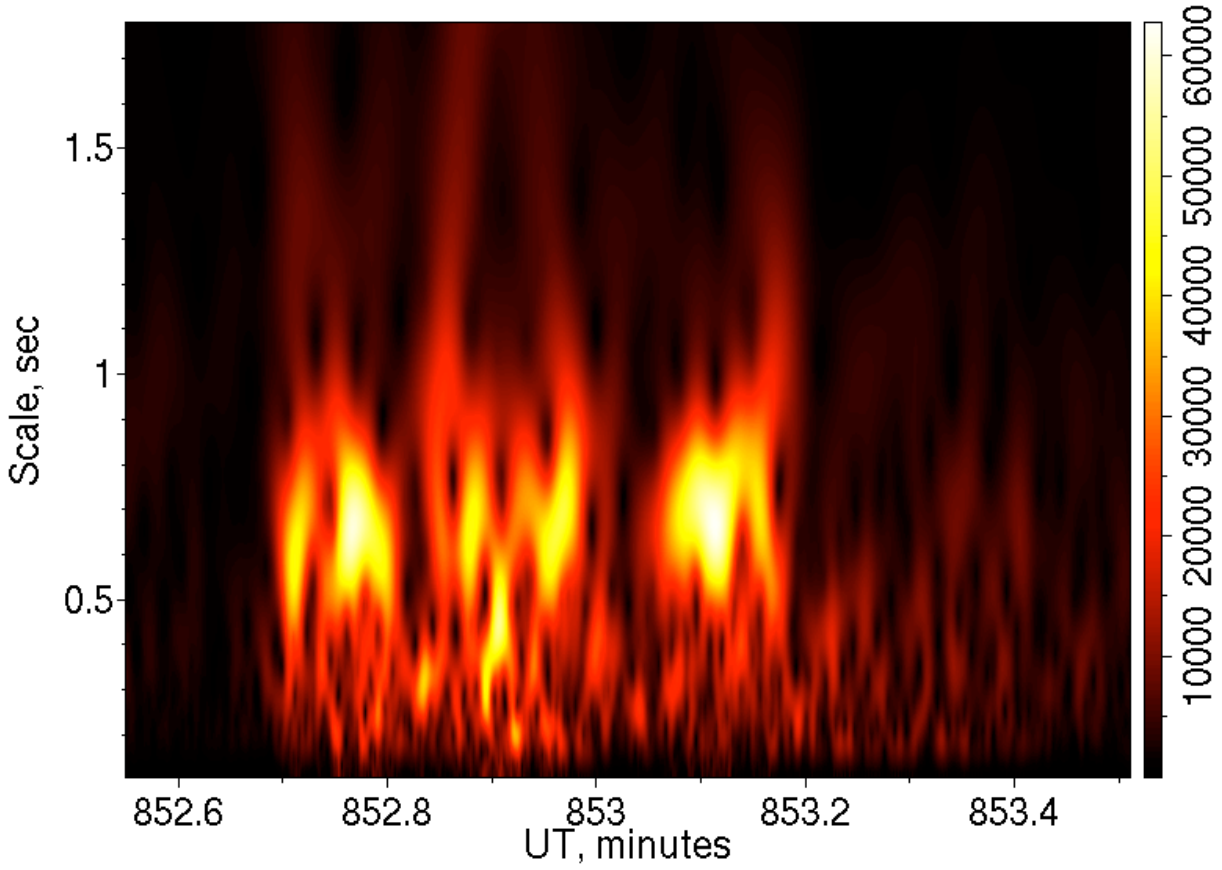

Ludwik Liszka

Swedish Institute of Space Physics

IRF Scientific Report 295

April 2008

Cover illustration:
Scalogram of the infrasonic signal from the Jokkmokk meteor, Kiruna, 2004-01-17.

Swedish Institute of Space Physics
Umeå

IRF Scientific Report 295
ISSN 0284-1703
ISBN 978-91-977255-4-5

Published by the Swedish Institute of Space Physics
Box 812
SE-981 28 Kiruna
SWEDEN
April 2008

LISTENING TO METEORS

Infrasonic Observations of Meteors in Northern Sweden

Ludwik Liszka

Swedish Institute of Space Physics
Umeå

IRF Scientific Report 295
ISSN 0284-1703
ISBN 978-91-977255-4-5

Published by the Swedish Institute of Space Physics
Box 812, SE-981 28 Kiruna, SWEDEN
April 2008

Preface

It is well known that the entry of bright bolides is usually associated with sound effects. During the past century it was discovered that a large part of the acoustic energy is radiated in the non-audible, low frequency part of the acoustic spectrum, or *infrasound*, known for its unusual propagation. Already in connection with the giant Tunguska Meteor in 1908, it was discovered that the low-frequency signal generated by the event travelled more than once around the Earth and was detected by barographs around the world. The presence of infrasound emissions from meteoroid entries was furthermore confirmed when infrasound became a common tool for detection of explosions. Several infrasonic observations of meteoroid entries are found in the literature. A pioneering work on the understanding of infrasound generation by meteoroid entry was done by Douglas ReVelle of Los Alamos National Laboratory.

When searching for meteoroid signatures, the original time series recorded by the infrasonic array is needed. Therefore, a systematic search for meteoroid signatures in the data from the Swedish Infrasound Network, SIN, could be started after 1994, when complete time series from the arrays were stored in a database. This book contains a summary of the work, performed by the author, on infrasonic detection of meteoroid entries above and around northern Scandinavia. Two major events occurred in northern Sweden during the past few years. These triggered the author's interest in documenting the events that have occurred there during the past century. The author is indebted to Mr. Per-Gunnar Jonsson, Skellefteå, for supplying all his collected materials about meteor events in Västerbotten during the past century and to Mr. Anders Persson, Sävar, for all information concerning the Hökmark-event, which constitutes the major part of Chapter 1.

The research described in this book was to a greater part made possible by the support from the European Space Agency, ESA, through the ESA Contract No. 19076/05/NL/PG. The author is indebted to Dr. Håkan Svedhem and Dr. Gerhard Drolshagen of ESA for their support and interest in this project.

The author is grateful to the ESRANGE Space Center for providing accurate position data for analyzed rocket launchings. The author is also indebted to Dr Esko Kyro, Finnish Meteorological Institute for supplying the radiosonde data from Sodankylä.

The study presented in this book would not have been possible without the help of my co-workers: Pär-Ola Nilsson, Jan Karlsson and Fredrik Rutqvist, who developed the software used in the operation of infrasonic arrays.

Table of Contents

Introduction

Large meteoroids enter the atmosphere with high supersonic speeds, typically between 10 and 75 km/sec. Since the Mach cone is very narrow at speeds of this order, the flight trajectory may be considered as a source of a cylindrical shock wave. At large distances, this shock wave will be transformed in to infrasound. During its travel through the atmosphere, the meteoroid heats up, due to friction, and undergoes fragmentation. The fragmentation may be of an explosive nature and a source of spherical shock. Sometimes a series of fragmentations may occur along the meteoroid's trajectory through the atmosphere. The total signature of a meteoroid entry will thus be very complex. It will be even more modified if the event is recorded at a large distance.

The most important parameter of an entry event is its kinetic energy, which depends on both the mass of the object and its speed. This is according to the method by ReVelle (1997), based on infrasound measurements of atmospheric nuclear tests:

$$\text{Log}(E/2) = 3.34 \log(P) - 2.58 \qquad (1)$$

where P is the period, in seconds, of the infrasound signal at maximum strength, and
E is the pre-atmospheric entry kinetic energy in kton TNT equivalent (1 kton TNT $\Leftrightarrow$ $4.185 \cdot 10^{12}$ J).

Another method to determine the total energy of the meteor is based on measurements of the pressure of the infrasound wave generated by the entry (ReVelle, 1997). Both methods usually give different results.

Attempts have been made to determine the last part of the meteor's trajectory using the infrasonic measurements (Le Pichon et al, 2002).
Northern Sweden was the scene of a few major meteor events during the past century. During the last three decades, infrasonic observations of meteoroid entries have been made possible by the Swedish Infrasound Network, which is important since few significant events have occurred above and around northern Scandinavia during that period.

One of the objectives of this book is to show what information about the meteoroid, and in particular about its orbit, can be extracted from infrasonic data for a few recent events over northern Sweden. An important question is: How much does the atmosphere, with its wind and temperature profiles, influence the entry signal?

A large fraction of meteor events is never reported. This may be due to weather conditions, or because events take place over oceans or uninhabited areas.

Another objective is to demonstrate a possible method for searching for unknown entry events in available infrasonic data. One must keep in mind that only events with a velocity component towards the observer can be detected using the infrasound.

References

Le Pichon, A., J.M. Guerin, and E. Blanc, Trail in the atmosphere of the 29 December 2000 meteor as recorded in Tahiti: Characteristics and trajectory reconstruction, *Journal of Geophysical Research*, **107**, D23, 4709, doi:10.1029/ 2001JD001283, 2002.

ReVelle, D. O.: 1997, Historical Detection of Atmospheric Impacts of Large Bolides Using Acoustic-Gravity Waves, Ann. NY Acad. Sci., in J. L. Remo (ed.), Near-Earth Objects- The United Nations International Conference, The New York Academy of Sciences, New York, New York, Vol. 822, pp. 284–302

Chapter 1

Historical Background

At least three major events were reported in northern Sweden before the infrasound data base started its operations in 1994, one in Kvavisträsk (1900) and one in Hökmark (1954). The third well-documented event was in Petikträsk (1988), not far from the previous impact locations.

Kvavisträsk

Kvavisträsk is a small village, about 130 km NNW from Umeå. The area is dominantly forests and farmland. A view over that part of the village where the meteor impact occurred is shown in Fig. 1.

Fig. 1. A view over the part of Kvavisträsk village where the meteor impact took place in 1900. Ludwig Lundgren, a victim of the event, lived in the old farmhouse visible on the photograph (photo by P-G Jonsson).

In the afternoon of May 20, 1900, Ludvig Lundgren (born 1845), see Fig. 2, went to see his neighbour, Fredrik on Berge. On his way along a meadow road, he was suddenly thrown down by a powerful explosion. A meteor struck the ground only 50 meters away from him. Neighbours found him unconscious on the road. He died of his injuries two days later, on May 22, 1900 without regaining consciousness.

The impact crater is still fully visible, more than 100 years after the event. The crater coordinates are: N64.9378 E19.6803. The view of the crater is shown in the photograph of Fig. 3. The crater is about 2 meters wide and 5 meters long. It is elongated in the NS direction, narrower at its southern edge, which may indicate that the meteor came from the south at a rather shallow angle. However, it is not certain that the form of the crater is the original one. According to the villagers, the crater was plundered by numerous meteorite-hunters during the 1930's.

This is probably the only documented case of a fatal injury connected with a meteor impact.

Fig. 2. Ludvig Lundgren (1845-1900) was killed by the impact of the Kvavisträsk-meteor on May 20, 1900 (the photo taken by a travelling photographer Hulda Nyberg, sometime before 1900).

Information about the Kvavisträsk-event may be found in the book: Qwafvisträsk by K. Johansson (in Swedish).

Fig. 3. The crater after the meteor impact in Kvavisträsk on May 20, 1900 (photo by P-G Jonsson).

Hökmark

Nearly fifty years later, another event took place not far from the previous one. The event was reported in a series of articles in the local newspaper Norra Västerbotten between June 10 and July 1, 1954.

In the evening of June 9, 1954, a considerable number of people across the area, more than 100 km wide, some 50 km south of the town of Skellefteå in northern Sweden, observed an object, larger than the full moon, coming down "like a lightning bolt", accompanied by a loud rumble. The time was just after 21:30 local time (which corresponds to 20:30 UT). Keep in mind that during the summer at these latitudes, it is still full daylight at this time of the day. The phenomenon was also seen on the Finnish side of the Golf of Bothnia. While playing in their yard in Hökmark, a small village 30 km south of Skellefteå, the brothers Bertil and Åke Petterson saw the flash that was shortly thereafter followed by swishing sounds and close impacts. A stone the size of a match-box landed 4 meters from the boys, which was cold when they picked it up from the ground. Another stone was found in the yard of the neighbouring house. Swishing sounds and impacts were heard in other parts of the village as well, indicating that the fragmentation of the meteor produced a large number of rather small fragments. 2 – 3 kilometers from the place where the two stones were found, there was apparently another area, about 70 meters in diameter, where a large number of small stone fragments fell on a meadow belonging to Johan Lundholm, a farmer in Hökmark.

The Swedish Museum of Natural History in Stockholm authorized the Boliden-geologist, Dr.David Malmqvist, to travel to Hökmark and acquire the two largest meteorites found in Hökmark for the Museum. The stones were purchased for 300 Swedish Crowns each, which was a considerable amount of money at that time. The stones were categorized as chondrites L4 and are still in the collections of the Museum. The Museum also gathered visual observations of the event and a preliminary orbit of the object was determined. The museum claims that only a small fraction of the object, perhaps from the first fragmentation, dropped over Hökmark. It was determined that the object entered the atmosphere from the north and continued further south after the Hökmark-event. However, there were no reports of similar events from villages south of Hökmark.

It is not known if other findings of meteorite fragments in Hökmark were ever investigated by experts.

This is not the end of the Hökmark story. In the middle of the 1990's, a person born in Hökmark, not long after the event, found a meteorite-like stone just 400 meters from the known impact site. Two photographs of the stone are shown in Fig. 4. The surface of the stone is black, showing clear traces of melting (left image). The stone is broken and the fracture shows a clear, layered structure (right image), which is never (according to some experts) observed in meteorites. The stone weighs 525g, with a density of >3 g/cm^3. The owner is reluctant to lend out the stone for scientific investigations. There are a few questions about this finding: Is that really a meteorite? Is there any relation between this finding and the Hökmark-event in 1954?

Fig. 4. A stone found in the mid 1990's, 400 m from the known impact area of the Hökmark meteorite.

Petikträsk

The event is described in the local newspaper, Norra Västerbotten, on May 27, 1988. A few days earlier, Mr. Gunnar Brännström discovered an elongated impact crater, 70 x 100 cm and 70 cm deep in the lawn of his summer house. Fragments of the lawn were thrown up to 50 meters in the direction of elongation of the crater. The grass on the fragments was still green, which indicates that the impact occurred no more than a week before it was discovered. After some digging, Mr. Brännström found two stones, probably meteorites. The smaller one, weighing 877 grams, was sent for examination to the Geological Survey of Sweden, the record of which is still archived. The sample was identified as a chondrite with a density of 2.85 g/cm^3 and a susceptibility of 0.03 SI-units. The fate of the second stone is not known. The position of the crater is N65.0561 E19.7392. The direction of orientation of the crater was not documented.

During the period of time when the event occurred, the infrasound array in Lycksele was in operation. However, during the years before 1994, only major events were processed and saved. Therefore, there is no way to confirm the event by means of infrasound data.

The above events, together with later ones, recorded by the Swedish Infrasound Network, are shown in Fig 5. There is a remarkable concentration of events in northern Västerbotten (a province of northern Sweden).

Meteor Events in Northern Sweden and Finland

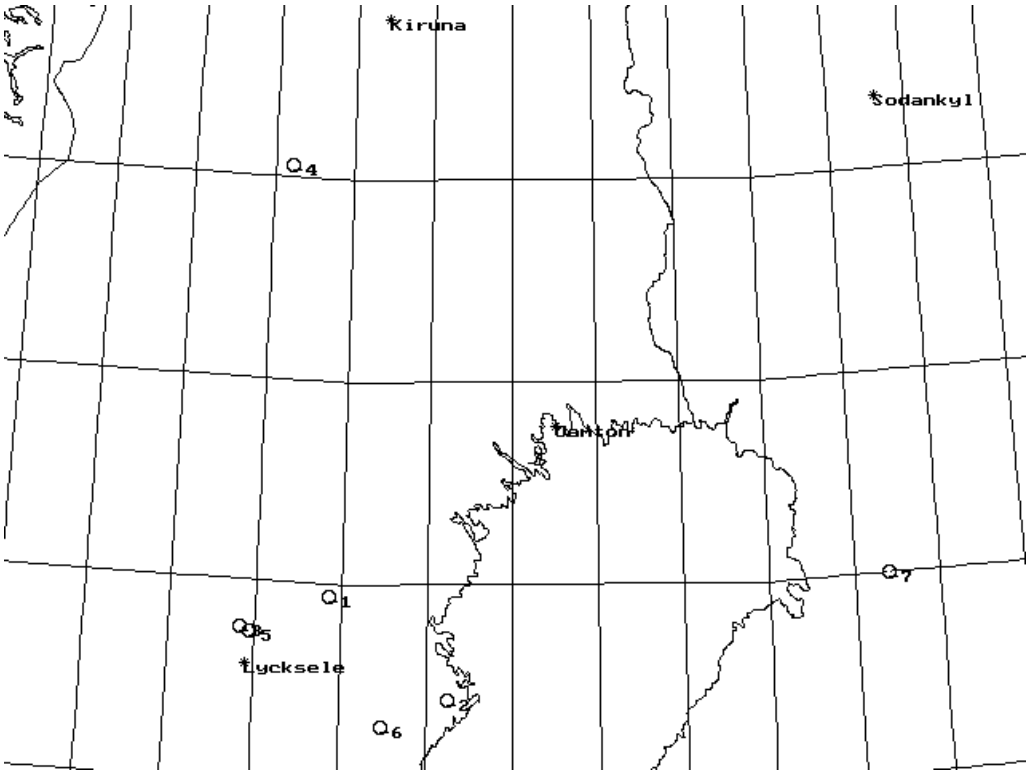

1. Kvavisträsk 1900-05-20 (one person killed)
2. Hökmark 1954-06-09
3. Petikträsk 1988-05-??
4. Jokkmokk 2004-01-17
5. Altarliden 2004-05-23
6. Bygdsiljum 2004-07-12
7. Oulu 2007-09-28

Fig. 5. Meteor events in northern Sweden and Finland

Reference to Chapter 1

Johansson K., Qwafvisträsk. Publisher: K. Johansson, Skellefteå 1998.

Chapter 2

Data Source for Meteor Observations

Since the beginning of the 1970's, the Swedish Institute of Space Physics (IRF) has operated four infrasound stations: Kiruna, Jämtön, Lycksele and Uppsala (see Fig. 6 and Table 1). All original time series collected since 1994 are stored in a data base accessible to the general public at the Internet home page for IRF, together with all standard software needed for data analysis. Each station consists of a tripartite microphone array located in the corners of an isosceles triangle, oriented in NS-EW directions. Microphones used in the network are unique, high sensitivity Lidström-microphones, manufactured in Sweden. Time series from all three microphones are stored in a compressed binary format, in 30-minute files.

In October 2006, the Uppsala-array was moved to Sodankylä, Finland, thus becoming a joint network effort between Sweden and Finland.

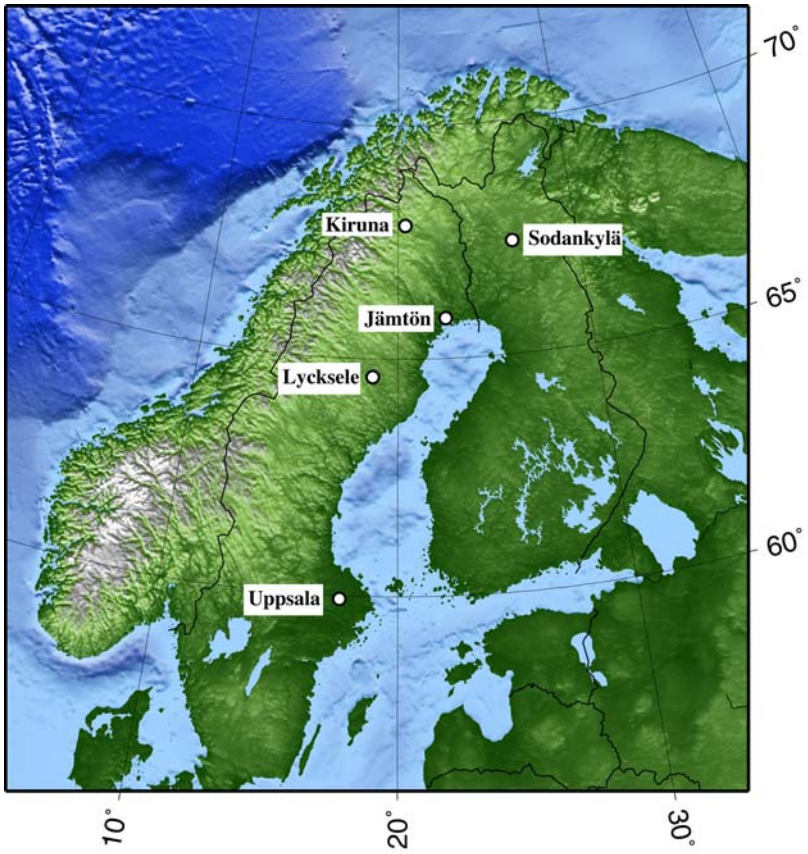

Fig. 6. Location of infrasound stations in Sweden and Finland.

Table 1. Stations in the Swedish-Finnish Infrasound Network (SIN)

Name	Latitude (Degs)	Longitude (Degs)
Kiruna	67.8˚N	20.4˚E
Sodankylä	67.42N	26.39E
Jamton	65.87˚N	22.51˚E
Lycksele	64.61˚N	18.71˚E
Uppsala	59.85˚N	17.61˚E

Basic Data Analysis

Background information

Files and file format

The entire day is divided into 48 30-minute files. Files are written in a binary format (.bin). Within the file data there are 512 samples blocks, each block containing the timing information and A/D readings from all 3 microphones. The sampling frequency is approximately 18 Hz, so that 32k samples (exactly 32,256) are obtained from each microphone during a 30-minute period. Time information in all files is the Internet-time (or in some stations, GPS-time) with an accuracy of about 0.1 sec.

File names:

For example: k5070830

Means:

k – Kiruna

5 - year 2005

07 - month July

08 - day 8th

30 - file no., starts at 1500UT

All data files may be downloaded from http://www.umea.irf.se/ when you select: Infrasound time series viewer

To process a **.bin** file type, the software: **crcorr.exe and crview.exe** will be needed. The software may be found on the above site under: *Locally developed software*. The time series are converted into the angle-of-arrival and trace velocity information typing, for example:

crcorr –c –t1 –s16 –g5 k5070830.bin

The time series analysis is based on a windowed cross-correlation analysis. The crcorr.exe generates the files k5070830.az and k5070830.caz. The .az-file is used mostly for viewing – it contains the complete information obtained during the analysis. The image produced by this software is usually not used. In order to view the file, type:

crview –t1 –g5 k5070830.az

The image contains one upper graph (angle-of-arrival, measured clockwise from N) and one lower graph (trace velocity in m/s being a measure of the angle of incidence). Since the entire graph is too large to fit in the screen, it is possible to move it with left/right arrows. The image may be saved as a **.png** graphic file by pressing "P" on the keyboard. The time in the bottom of the graph is expressed in UT minutes and seconds. There are distributions of observed azimuths on the left and right side of the azimuth graph. The inner distribution depicts the raw azimuth readings, the outer is a weighted (with the cross-correlation between microphones) distribution. Vertical lines on the graph are the result of an automatic signal detector at its default settings, which may be adjusted. Information about all available switches and functions can be obtained by typing the software name without any switches. All software must be executed in a DOS-window.

.caz-file may be used for further data processing. Columns in the file are:

1. **Time:** UT in minutes and decimals
2. **Angle-of-arrival:** in degrees, measured clockwise from North.
3. **Trace velocity:** in m/sec (velocities < speed of sound correspond to local pressure fluctuations and should be discarded).
4. **A:** the average amplitude in A/D readings for all 3 microphones.
5. **Cr:** the product of all 3 cross-correlation coefficients between 3 microphone pairs. If Cr < 0.008, all 3 correlation coefficients are, on average, < 0.2 and the reading, most likely, represents noise.
6. **A*Cr:** the product of the amplitude and the cross-correlation coefficients product.

Results of analysis showing both the azimuth and the trace velocity may be stored in .png files by pressing the key "P".

The software **il2tmseries.exe** may be used to convert .bin files into ASCII time series files. This software is also available at the above html-address.

Main Tasks of the Study

This study may be divided into the following steps:

1. Test of the method of analysis

In order to understand the results of infrasonic observations of meteor impacts, observations of re-entries of high altitude rockets may be used. Such a re-entry is similar to an impact of a meteoroid.

2. Results of observations of a few significant meteor impacts in northern Scandinavia and its surroundings.

The same method of analysis that is used for observations of rocket re-entries is applied to four major meteor impacts.

3. Extraction of orbital information

What kind of orbital information can be obtained from infrasonic multi-station observations?

4. Update of the method for automatic recognition of signals from meteor events (Liszka 2003) using data from all meteor events recorded by the SIN.

The previous method was based on the Principal Component Analysis (PCA) of multiple indicator data. Indicators are distributions of variables within a given analyzing window:

Angle-of-arrival

Horizontal phase velocity

Cross-correlation across the array
Spectral slope
In this study, a neural network (NN) categorizing technique was used instead of the PCA method.

5. Search for infrasound data of meteor events north of and in the neighbourhood of Scandinavia during 1994 – 2004.

The method, based on infrasonic observations of known entry events during the recent years, results in a first screening of the entire accumulated data from SIN stations (a total of about 200 Gbytes of data). The first list of potentially possible events is a subject of further screening with respect to events location, speed determination, flight direction and other event parameters.

6. Analysis of high trace velocity events.

Two minor meteor events, observed by only one station, were found to be associated with signals with very high horizontal trace velocities across the array (being a measure of the source elevation). In these cases, there is an indication that the sources were nearly overhead. Their spectral content (lack of high frequencies) may also indicate a great source height.
Unexplained signals with very large amplitudes and high horizontal trace velocities are occasionally observed at SIN stations. Many of these signals were once discarded, assuming being a result of local interferences. Here, we carry out a systematic search for these events.

Chapter 3

Infrasonic Observations of

Re-entries of High Altitude Rockets

Re-entry of spacecrafts may generate, if the entry velocity is great enough, infrasonic signals similar to those produced by meteor impacts. ReVelle et al. (2005) analyzed a hypersonic impact of the space capsule Genesis over the Utah desert. The object approached the Earth's surface at a shallow angle of 8 degrees and at a speed of 11 km/sec. The event was monitored and analyzed as a low-velocity meteor. In this chapter, the re-entries of the high-altitude sounding rockets *Castor 4B* and *Skylark 7*, launched at the ESRANGE Space Center outside Kiruna, Sweden, are analyzed. Observations were performed from three infrasonic arrays in northern Sweden, belonging to the Swedish Infrasound Network (see Table 1).

In spite of much lower entry velocities (2.8 resp. 1.8 km/sec), the fall through the atmosphere was nearly vertical and thus easy to interpret. The Castor 4B rocket reaches the height above 700 km while Skylark 7 only about 250 km. Information about both rockets is presented in Table 2. The accurate positioning data for each second of flight was supplied by ESRANGE.

Table 2. Sounding rockets

	Castor 4B	Skylark 7
Length, m	8.8	7.6
Diameter, m	1.02	0.44
Max. altitude, km	>700	~250
Max. descent velocity, km/sec	2.8	1.8

During the descent of the rocket, the velocity increases until the atmospheric drag is great enough to start its decrease. While at supersonic descent velocity, the rocket will be a source of a cylindrical shock. The wave-normal of the shock is inclined to the ground plane by the angle 90 - , where θ is the Mach angle, see Fig. 7. Unlike meteor impacts, the re-entry of a rocket generates only a cylindrical shock, without explosions along its trajectory.

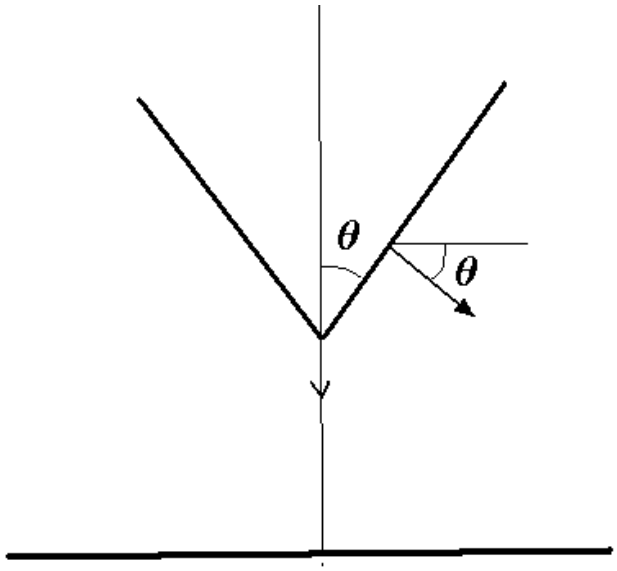

Fig. 7. Vertical impact with a shock cone and the Mach angle θ.

When the altitude of the rocket decreases, the atmospheric drag causes a decrease in the velocity of the rocket. The propagation angle with respect to the horizontal plane,θ, (see Fig. 7) increases with the decreasing altitude. The variation of θ with the height for both rocket types is shown in Fig. 8a and b.

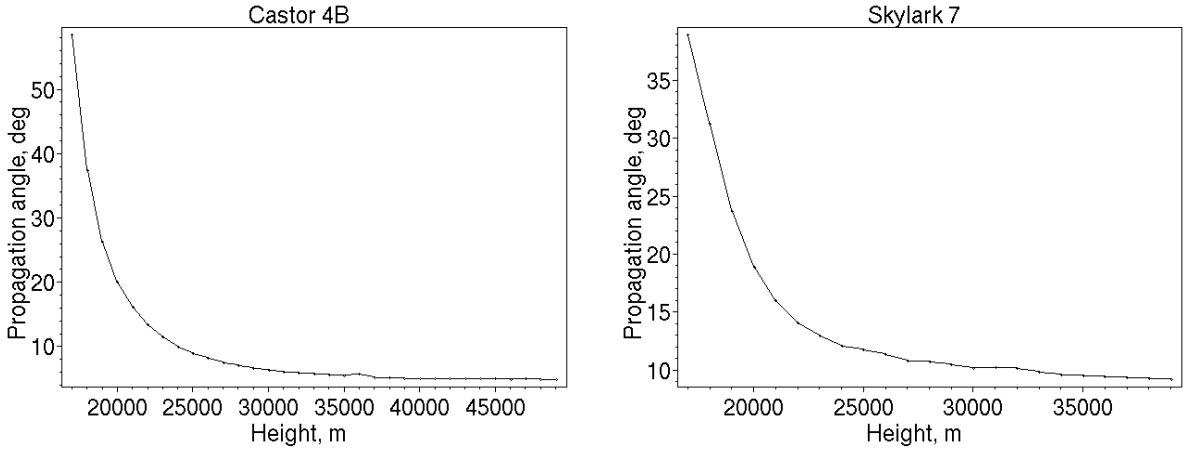

Fig. 8. The propagation angle,θ, as a function of rocket altitude for Castor 4B (a) and Skylark 7 (b).

The approximate average position of the impact area is N 68° 40’ E 20° 40’.

Table 3. Rocket launchings recorded at different arrays.

Rocket	Date	Kiruna	Jämtön	Lycksele
Castor 4B	1998-11-24	x	-	x
”	2001-04-29	x	x	x
”	2003-04-01	x	-	x
”	2004-11-22	x	x	X
”	2006-05-02	x	x	x
Skylark 7	2004-12-02	x	x	x
”	2005-12-01	x	-	-
”	2006-05-11	x	x	-

Explanation of symbols: x signal detected
- No signal detected

Table 4. True directions and distances from different arrays.

Name	Direction (Degrees)	Distance (km)
Kiruna	6.5	92
Jämtön	346.6	319
Lycksele	10.0	456

Data analysis

Time series from each array are frequency-filtered using a set of wavelet filters. The list of filters is given in Table 5.

Table 5. List of wavelet filters

Frequency band #	Frequency, Hz	Type of filter	Centre frequency, Hz
1	<1	Low-pass	.75
2	1 – 2	Band-pass	1.5
3	2 – 3	“	2.5
4	3 – 4	“	3.5
5	4 – 5	“	4.5
6	>5	High-pass	5.5

Since the microphone signal is band-pass filtered between 0.5 and 6 Hz, centre frequencies of channels 1 and 6 may be estimated to 0.75, respective 5.5 Hz.

For each frequency channel, the angle-of-arrival and the horizontal trace velocity were calculated using the cross-correlation technique. A description of the procedure and the software used may be found at: http://www.umea.irf.se/iltserie/quick-tutorial.php. The narrow-band analysis increases the azimuth and trace velocity resolution and is used

throughout the entire study. Different frequency bands are plotted on the angle-of-arrival and trace velocity graphs with different sizes of circles, the smallest for the lowest frequency.
Graphs showing calculated angle-of-arrival and trace velocity from all three arrays and for all eight analyzed rocket re-entries are shown in Figs. 9 – 16 (two upper rows of graphs).
In order to clearly show the distribution of observed angle-of-arrival, the data was time-averaged and histograms for each frequency band were calculated. Results are shown in the third row of graphs in Figs. 9 –16.

In order to compare the observed signal characteristics with atmospheric conditions, the sound velocity profile (left) together with zonal (middle) and meridional (right) winds over northern Finland at noon are shown in the bottom graphs (source: Finnish Meteorological Institute) up to 25000 m. Positive direction of the zonal wind is towards W, and of the meridional wind towards S.

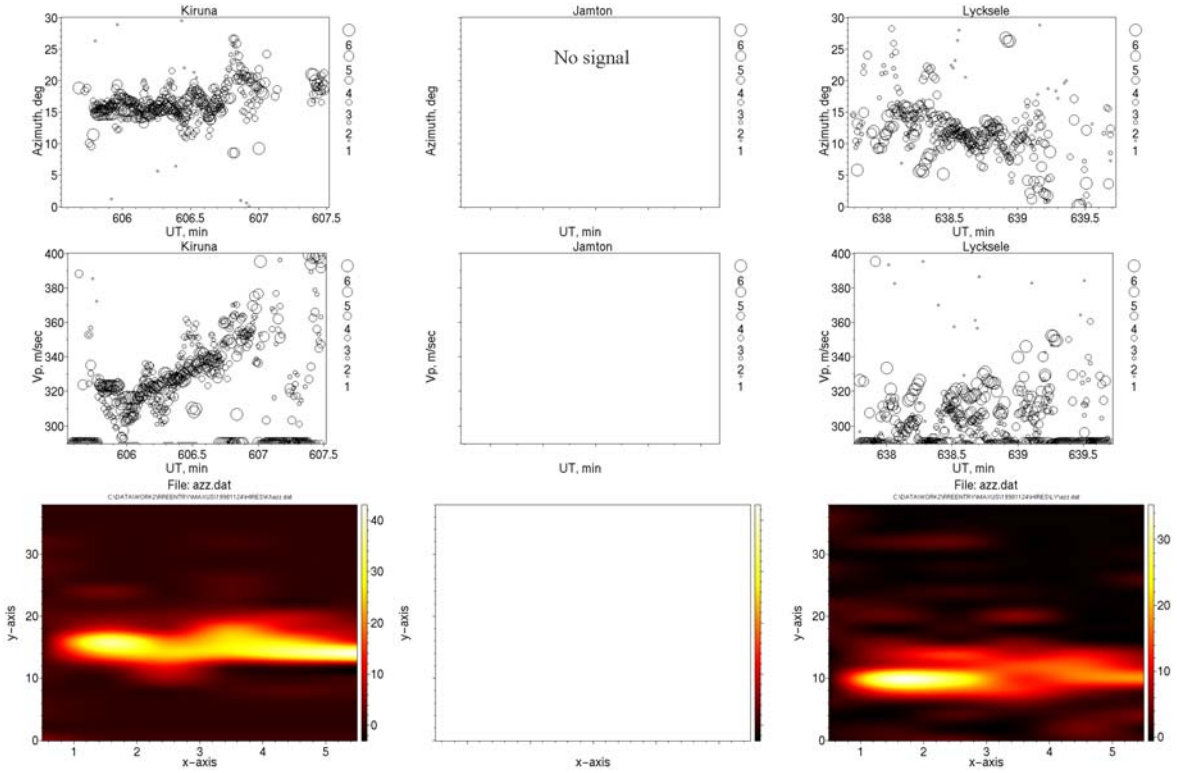

Sodankylä-radiosonde atmospheric data

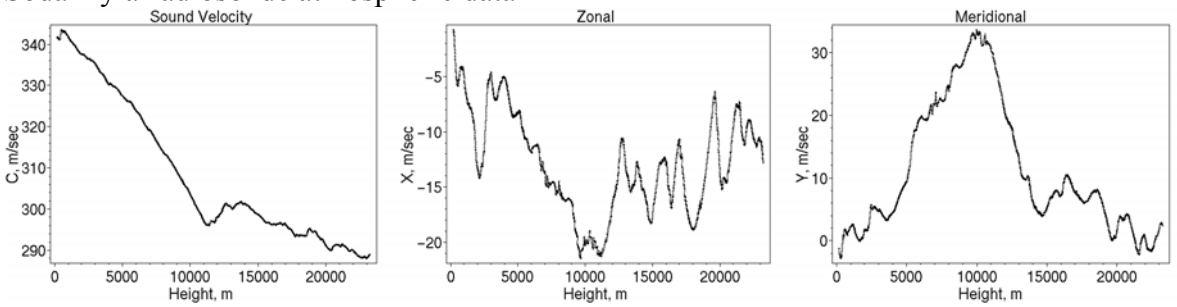

Fig. 9. Castor 4B re-entry, 1998-11-24. Top row: angle-of-arrival, second row: horizontal trace velocity. Third row: time-averaged histograms of the angle-of-arrival as a function of frequency. No signal detected at the Jämtön-array. The bottom graphs: sound velocity (left), zonal (middle) and meridional (right) winds over northern Finland at noon (source: Finnish Meteorological Institute) up to an altitude of 25,000 m. Positive direction of the zonal wind is towards W, and of the meridional wind towards S.

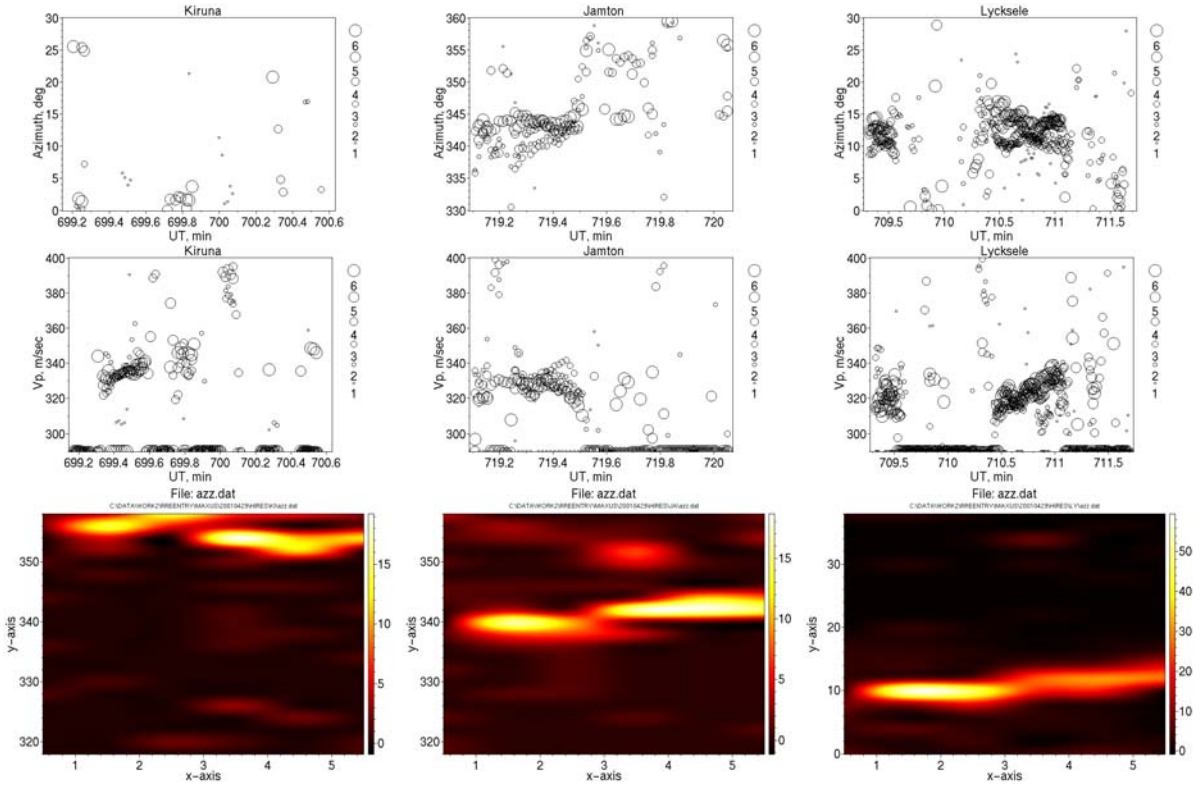

Sodankylä-radiosonde atmospheric data

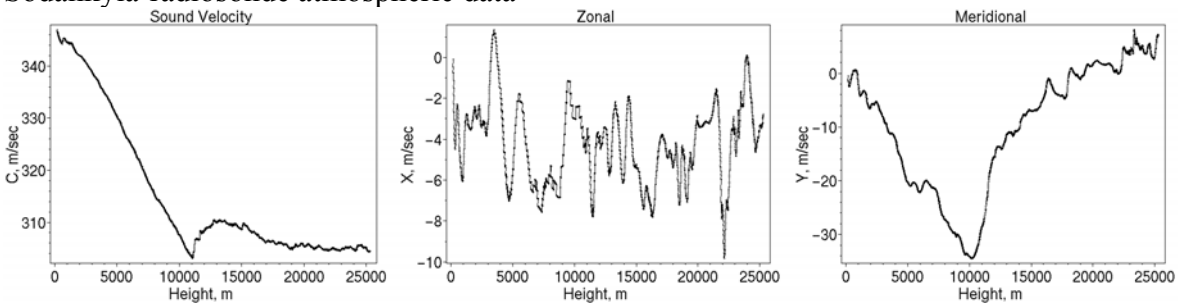

Fig. 10. Castor 4B re-entry, 2001-04-29. Top row: angle-of-arrival, second row: horizontal trace velocity. Third row: time-averaged histograms of the angle-of-arrival as a function of frequency. The bottom graphs: sound velocity (left), zonal (middle) and meridional (right) winds over northern Finland at noon (source: Finnish Meteorological Institute) up to an altitude 25,000 m. Positive direction of the zonal wind is towards W, and of the meridional wind towards S.

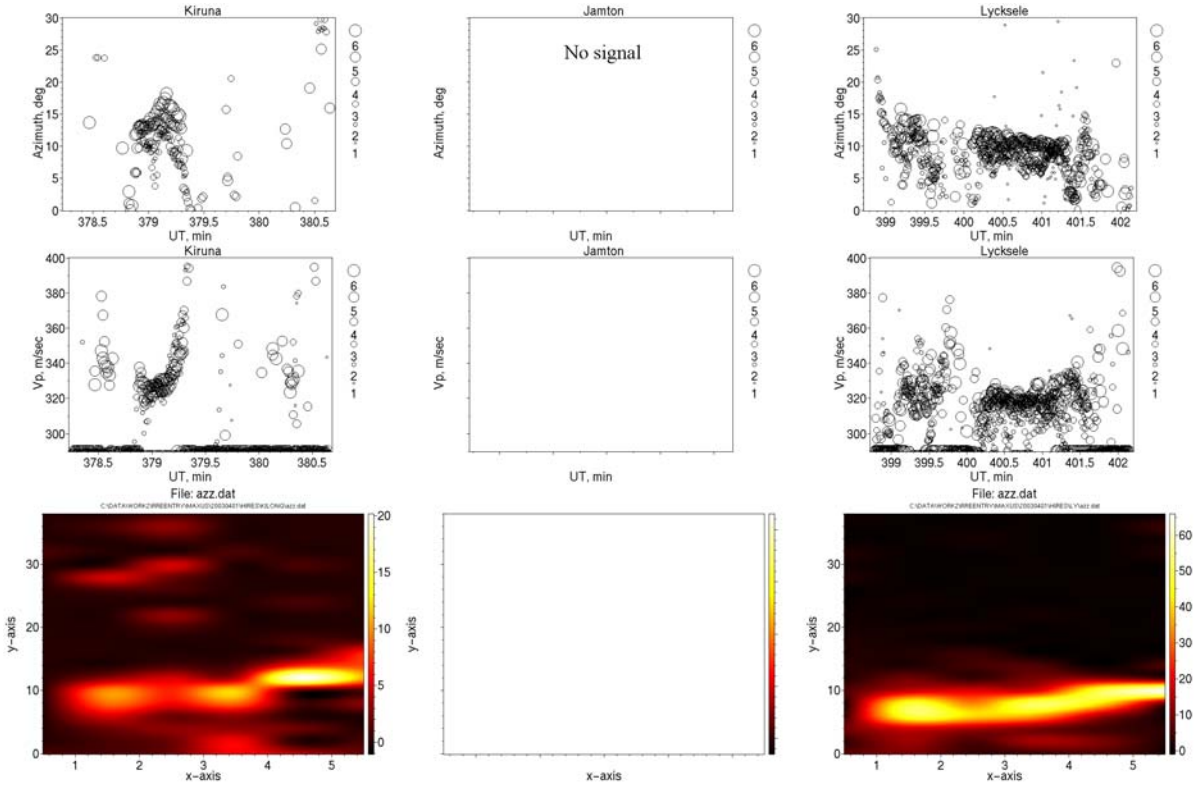

Sodankylä-radiosonde atmospheric data

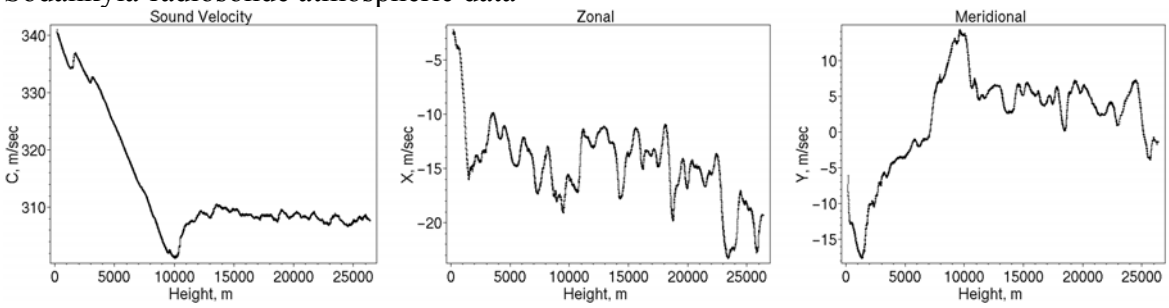

Fig. 11. Castor 4B re-entry, 2003-04-01. Top row: angle-of-arrival, second row: horizontal trace velocity. Third row: time-averaged histograms of the angle-of-arrival as a function of frequency. No signal detected at Jämtön-array. The bottom graphs: sound velocity (left), zonal (middle) and meridional (right) winds over northern Finland at noon (source: Finnish Meteorological Institute) up to an altitude of 25,000 m. Positive direction of the zonal wind is towards W, and of the meridional wind towards S.

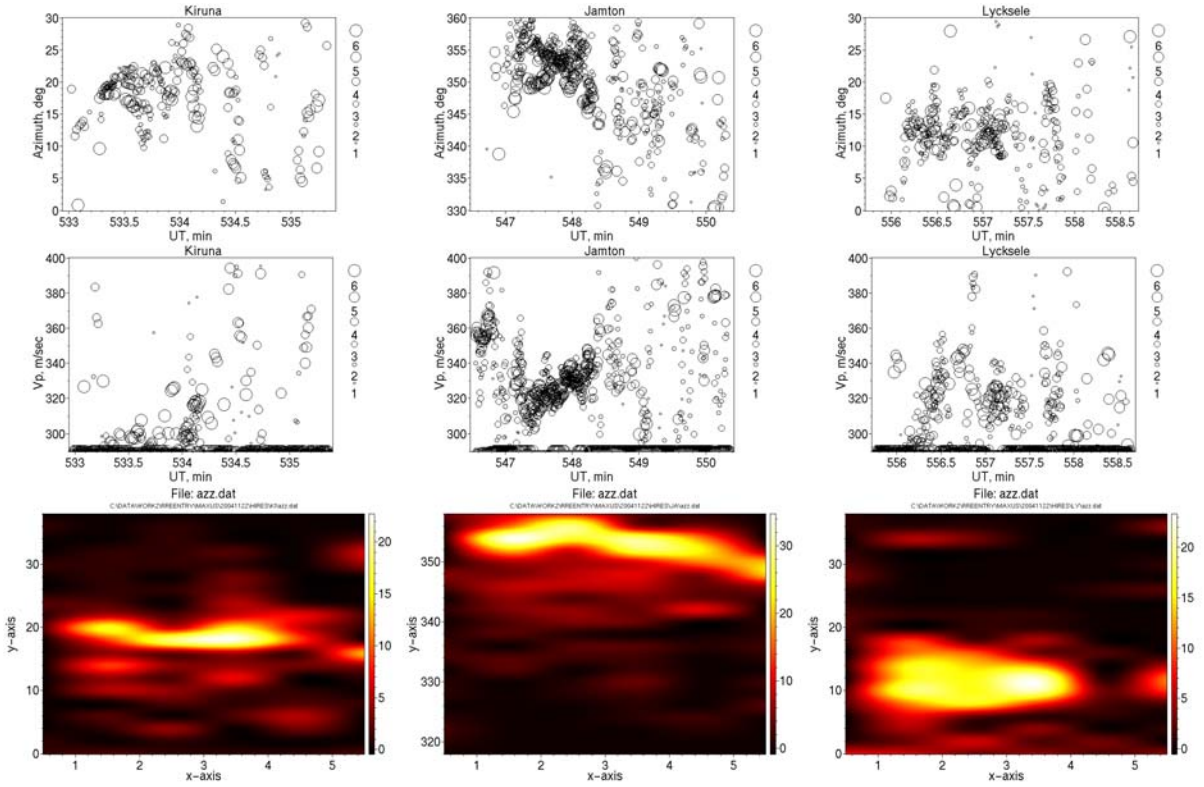

Sodankylä-radiosonde atmospheric data

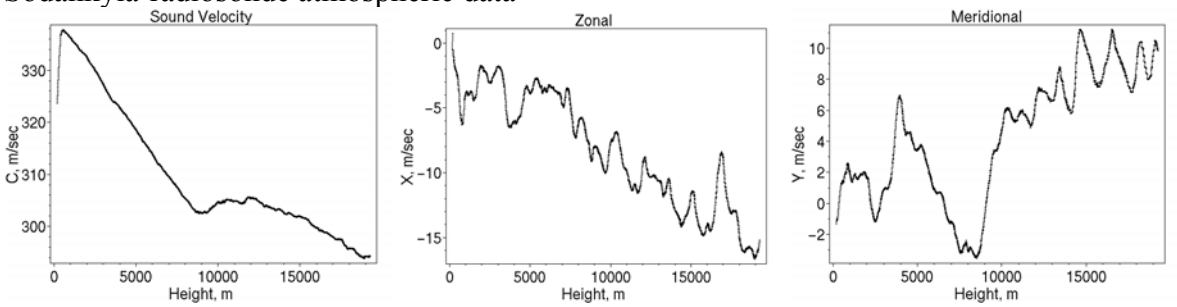

Fig.12. Castor 4B re-entry, 2004-11-22. Top row: angle-of-arrival, second row: horizontal trace velocity. Third row: time-averaged histograms of the angle-of-arrival as a function of frequency. The bottom graphs: sound velocity (left), zonal (middle) and meridional (right) winds over northern Finland at noon (source: Finnish Meteorological Institute) up to an altitude of 20,000 m. Positive direction of the zonal wind is towards W, and of the meridional wind towards S.

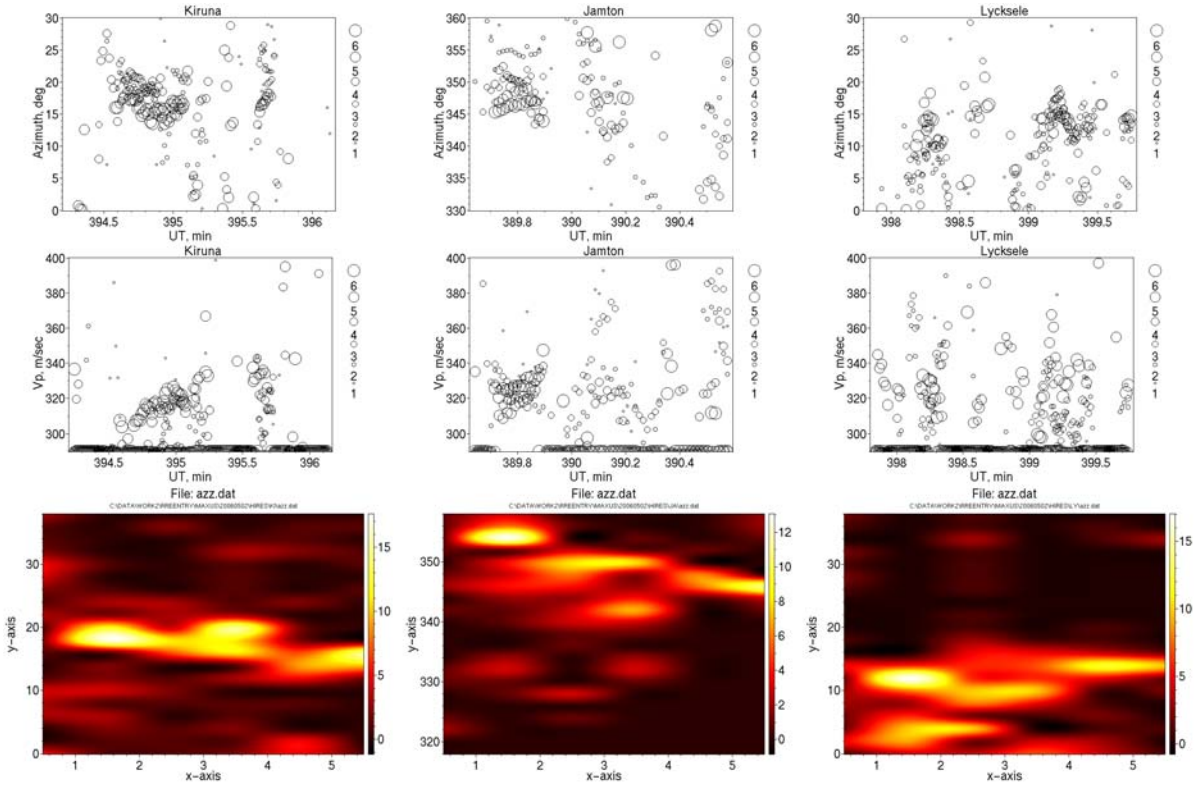

Sodankylä-radiosonde atmospheric data

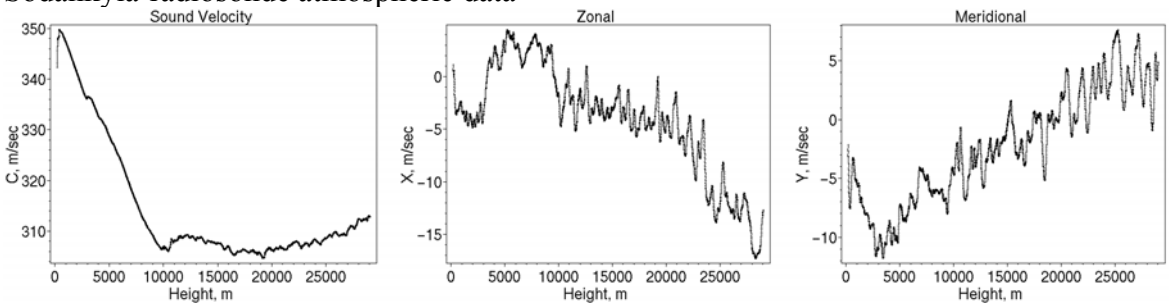

Fig.13. Castor 4B re-entry, 2006-05-02. Top row: angle-of-arrival, second row: horizontal trace velocity. Third row: time-averaged histograms of the angle-of-arrival as a function of frequency. The bottom graphs: sound velocity (left), zonal (middle) and meridional (right) winds over northern Finland at noon (source: Finnish Meteorological Institute) up to an altitude of 30,000 m. Positive direction of the zonal wind is towards W, and of the meridional wind towards S.

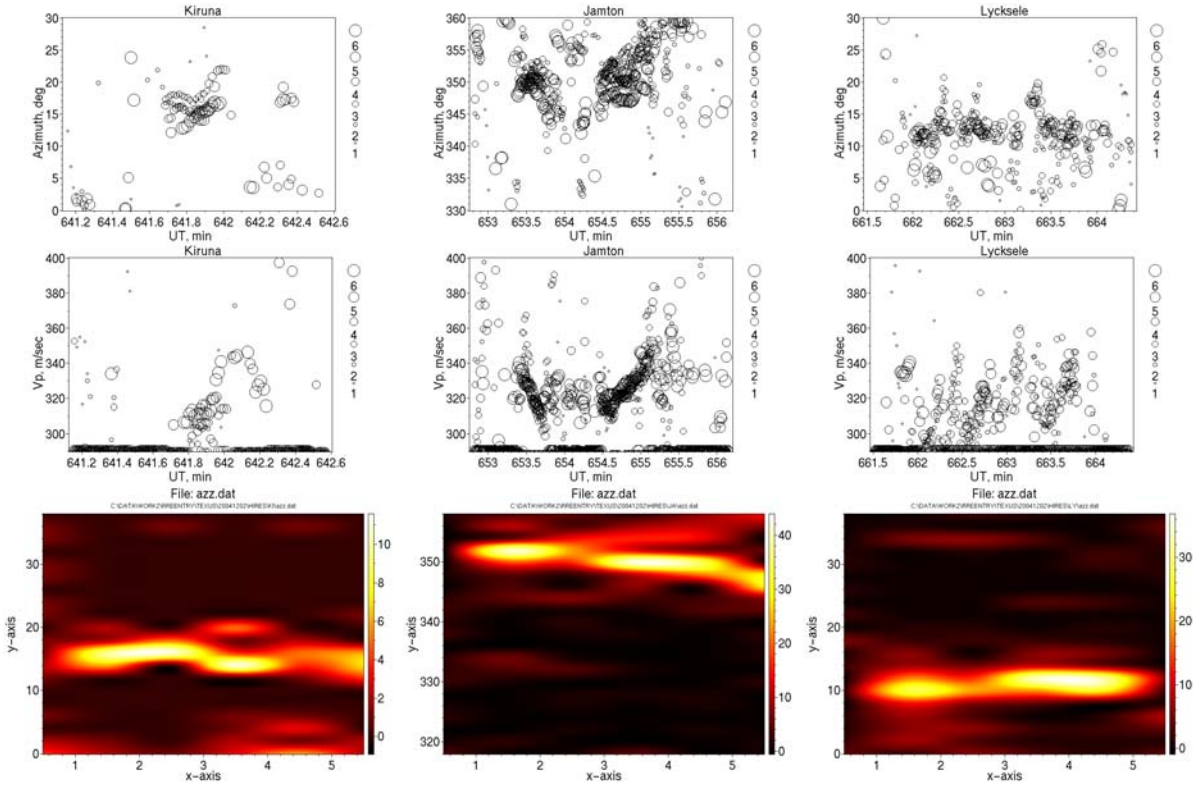

Sodankylä-radiosonde atmospheric data

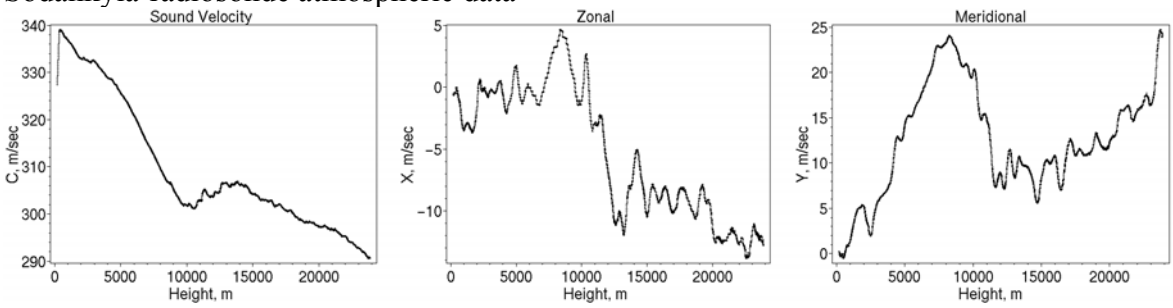

Fig. 14. Skylark 7 re-entry, 2004-12-02. Top row: angle-of-arrival, second row: horizontal trace velocity. Third row: time-averaged histograms of the angle-of-arrival as a function of frequency. The bottom graphs: sound velocity (left), zonal (middle) and meridional (right) winds over northern Finland at noon (source: Finnish Meteorological Institute) up to an altitude of 25,000 m. Positive direction of the zonal wind is towards W, and of the meridional wind towards S.

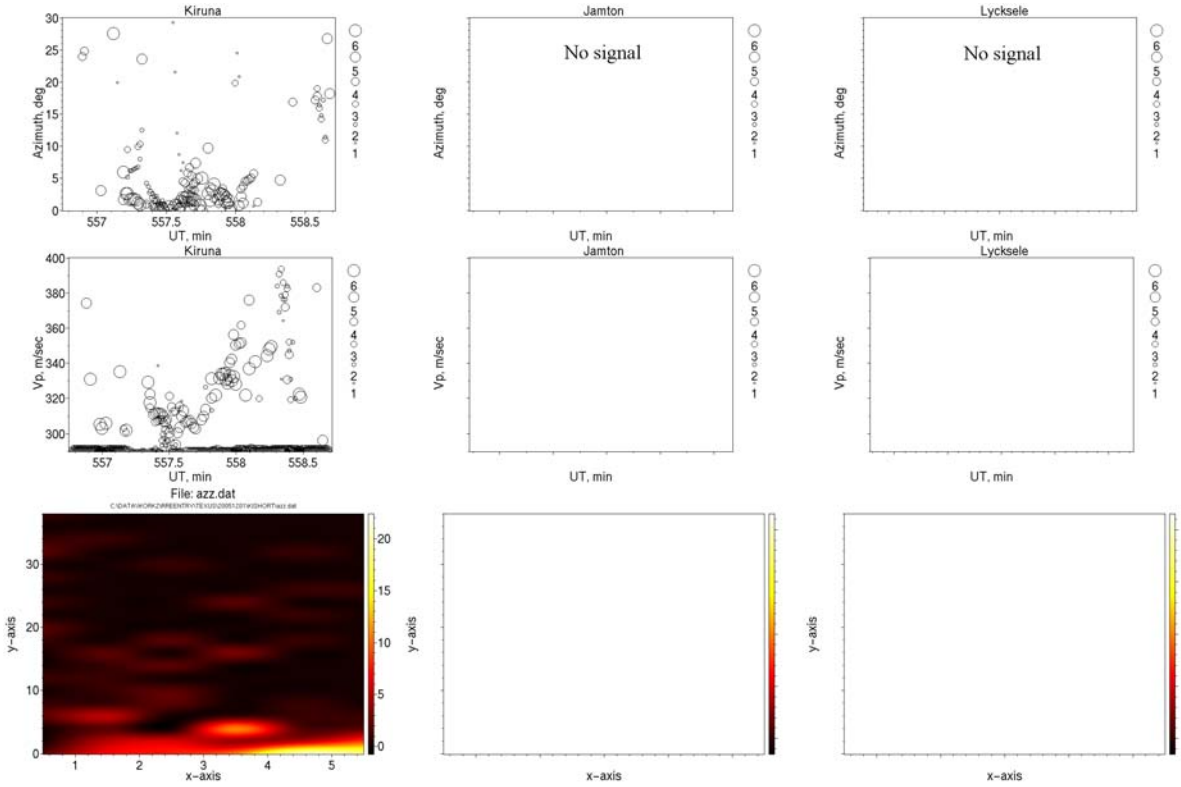

Sodankylä-radiosonde atmospheric data

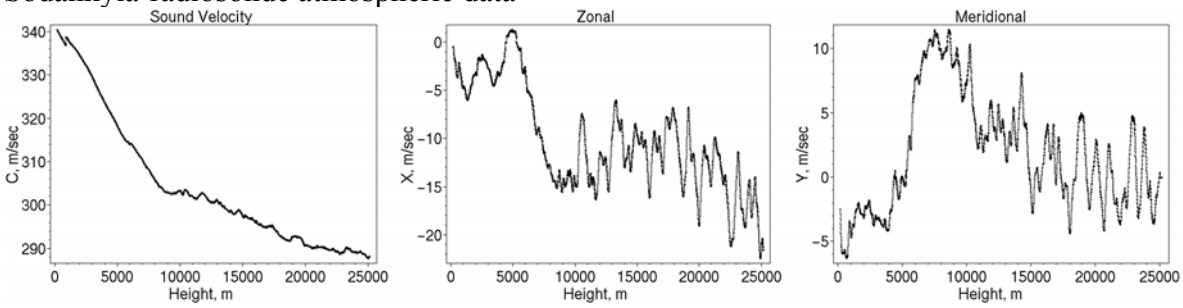

Fig. 15. Skylark 7 re-entry, 2005-12-01. Top row: angle-of-arrival, second row: horizontal trace velocity. Third row: time-averaged histograms of the angle-of-arrival as a function of frequency. No signal detected at Jämtön- and Lycksele-array. The bottom graphs: sound velocity (left), zonal (middle) and meridional (right) winds over northern Finland at noon (source: Finnish Meteorological Institute) up to an altitude of 25,000 m. Positive direction of the zonal wind is towards W, and of the meridional wind towards S.

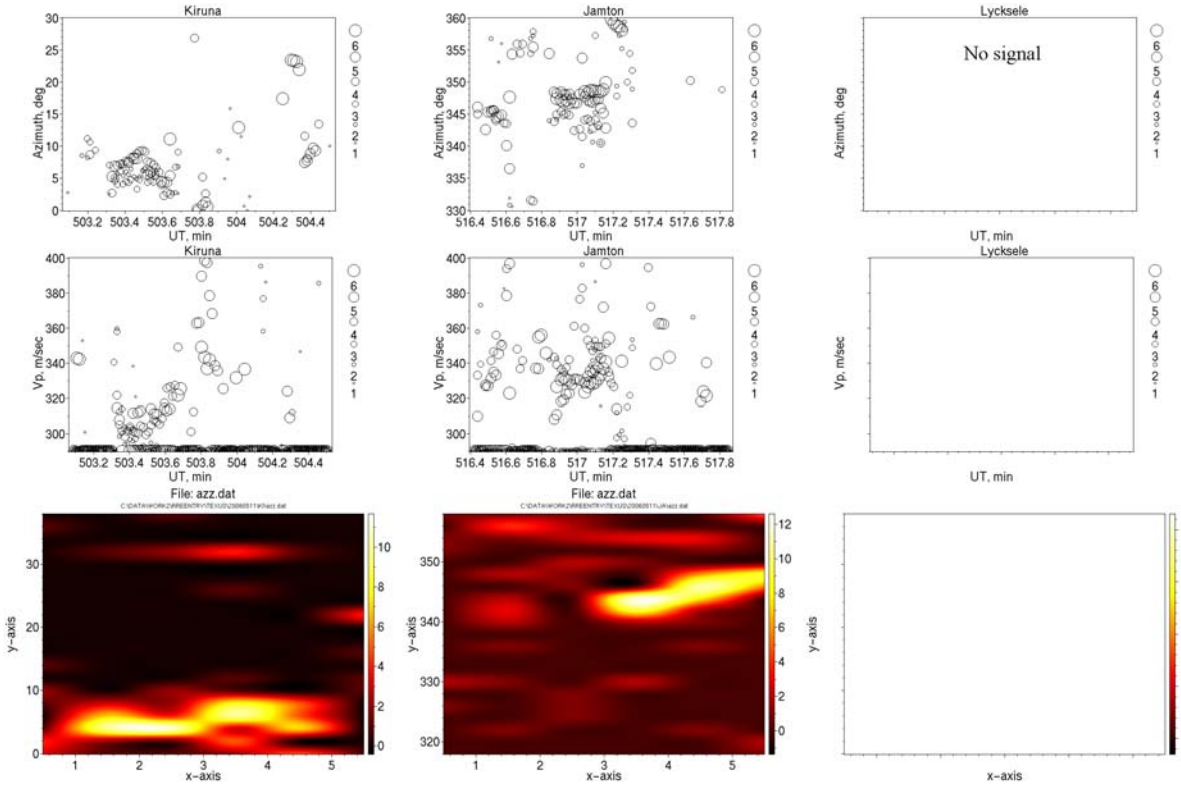

Sodankylä-radiosonde atmospheriwind data

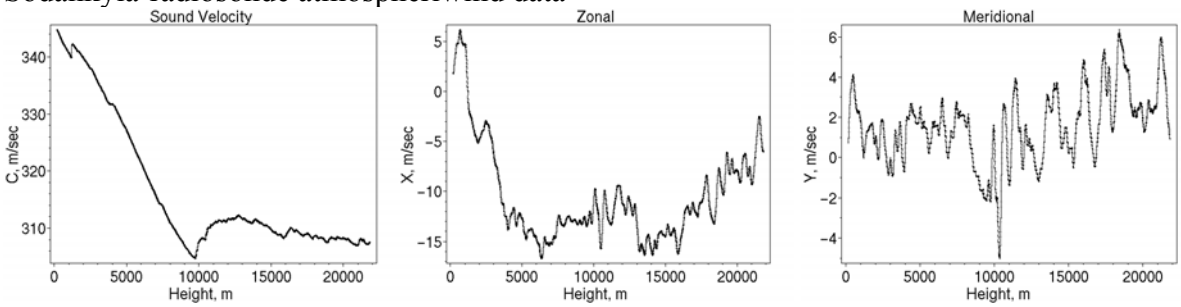

Fig. 16. Skylark 7 re-entry, 2006-05-11. Top row: angle-of-arrival, second row: horizontal trace velocity. Third row: time-averaged histograms of the angle-of-arrival as a function of frequency. No signal detected at Lycksele-array. The bottom graphs: sound velocity (left), zonal (middle) and meridional (right) winds over northern Finland at noon (source: Finnish Meteorological Institute) up to an altitude of 25,000 m. Positive direction of the zonal wind is towards W and of the meridional wind towards S.

Discussion of Graphs

A visual inspection of the graphs leads to following conclusions:

- Angle-of-arrival and horizontal trace velocity (two upper rows of graphs in Figs. 9 – 16) show rapid, irregular variations in time as well as a large spread of data points. This is also the case for the closest array in Kiruna, only 92 km from the source. This indicates substantial irregularities in both the wind and temperature distributions.
- Castor 4E (the larger rocket) generates signals with a longer duration (and amplitude) than Skylark 7.
- Double arrivals are observed on several occasions at all arrays.
- Distributions of the angle-of-arrival (displayed in the third row of graphs) show that the horizontal propagation varies strongly with the wave frequency. The most complex structure of distributions was observed on May 5, 2006 at all arrays. Remarkably, large lateral deviation (>20 degrees) of signals recorded in Kiruna was observed on April 29, 2001 during a Castor 4E launch. At the same time, radiosonde measurements over northern Finland indicate a strong (35 m/sec) northerly wind at the tropopause.
- Simultaneous wind- and temperature radiosonde measurements over northern Finland show, in most cases, a lot of structures/irregularities up to the highest altitude of operation (35 km).

A Propagation Model

Assuming a conventional summer model of sound velocity and wind profiles in the atmosphere, it can be seen from ray-tracing calculations (see Fig. 17) that no signal should reach the ground level at a distance corresponding to position of the Kiruna-array.

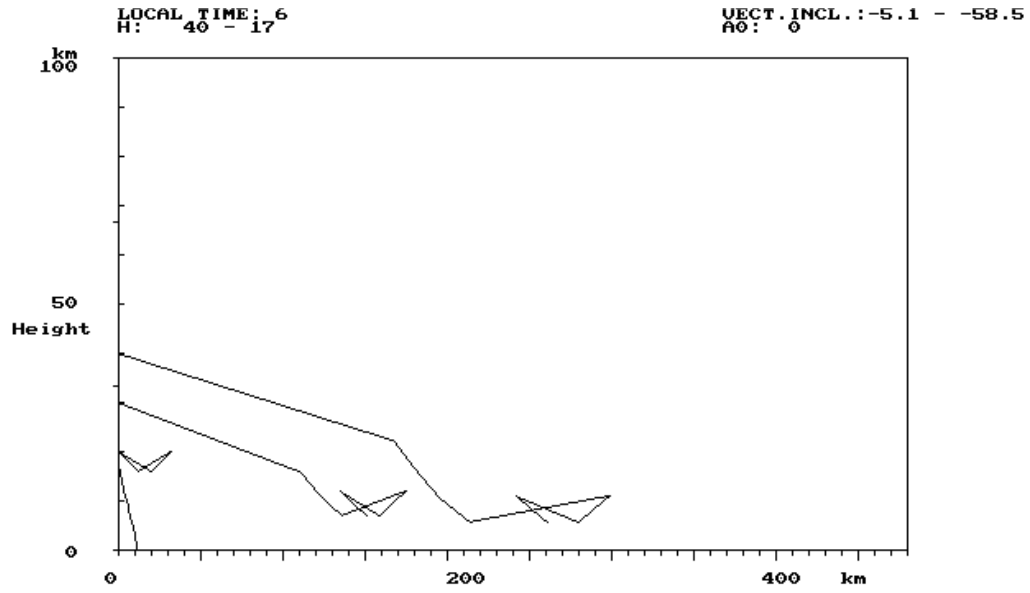

Fig. 17. Propagation of sound waves during the descent of a Castor 4E rocket. The lowest ray originates at the lowest supersonic altitude of 17 km. All rays originating at heights above 18 km will be dissipated after reflection from the top of the tropopause.

Only rays originating close to the lowest supersonic height will reach the ground level within a radius of about 20 km around the entry point. Obviosly, observation results do not agree with ray-tracing calculations using a conventional model.

Interesting observations may be made by studying the wavelet spectrum (scalogram) of the recorded signal:

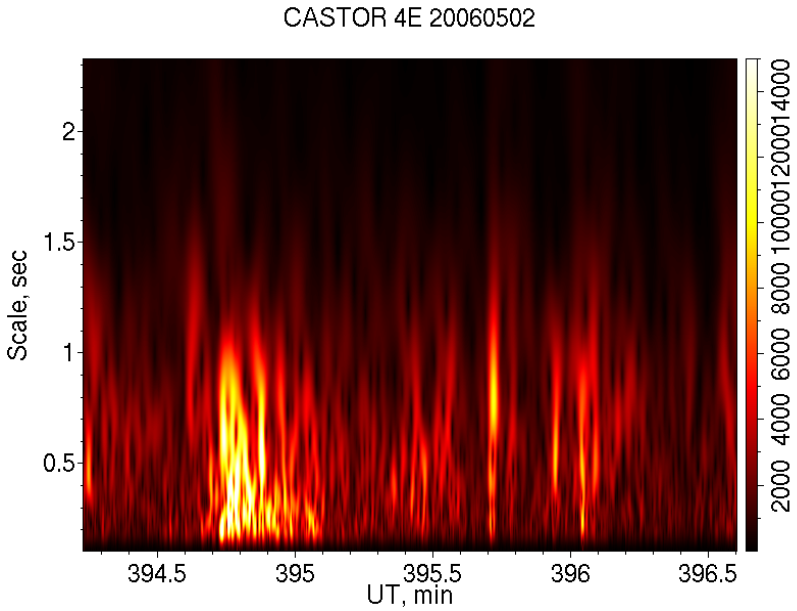

Fig. 18. The scalogram of signals from the Castor4E re-entry on May 2, 2006 (Unfiltered signal).

As shown, the recorded signal consists of a large numbers of wave packets with slightly different frequencies (scales) and different arrival times. It is plausible to assume that the different signal packets arrive from different heights after reflection from individual atmospheric irregularities in wind and/or temperature. The diversity of propagation paths implies that the order of arrivals to the array may be very different from the order at which the signal packets were generated along the re-entry trajectory.

Adding randomly-distributed irregularities in wind and/or temperature to a conventional, smoothed atmospheric model, more realistic ray-tracing results can be obtained (Liszka, 1997). A graph corresponding to Fig. 17 is obtained (see Fig. 19).

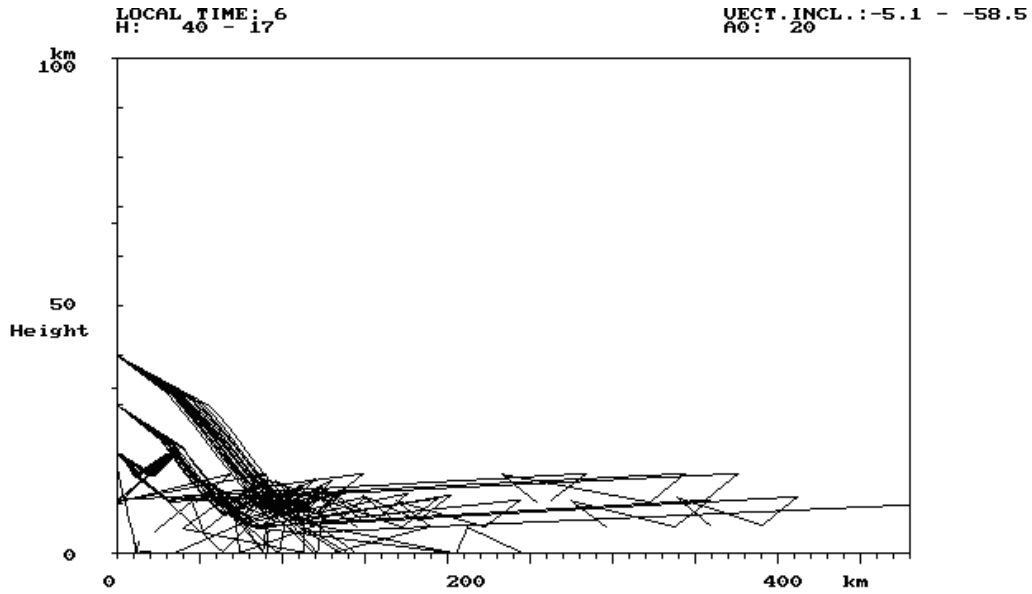

Fig. 19. Propagation of sound waves during the descent of a Castor 4E rocket. The lowest ray originates at the lowest supersonic altitude of 17 km, the atmospheric model with Gaussian-distributed irregularities in wind and temperature is used. A large fraction of the rays that originated at heights above 18 km now reach the ground.

It is apparent that the introduction of irregularities into the atmospheric model yields a realistic result. Evidently, signals from the re-entries are almost always recorded at all arrays.

Further Data Analysis

The main question is whether it is possible, from infrasonic observations, to draw conclusions about the entry velocity and direction.

It is now assumed, based upon visual inspection of many years of infrasonic signals, that at short ranges (<100 km), the horizontal trace velocity (Vp) is less influenced by propagation effects than the angle-of-arrival (AA) and the time-of-arrival (TA). Since Vp is related to the height at which the signal was generated, the straightforward consequence of the above assumption is, that the data triplets (TA, AA, Vp) from one event have to be sorted with respect to Vp. The data is then a subject of a simple statistical analysis:
The median of Vp, Vpm is calculated.

The data set is divided into two subsets: subset 1 with Vp<Vpm and subset 2 with Vp>Vpm. Median values and standard deviations are calculated for TA, AA and Vp for both subsets.
The procedure results in two sets of medians:
TAm1, AAm1, Vpm1 TAm2, AAm2, Vpm2
And two sets of standard deviations, being measures of data scatter within each subset:
TAsd1, AAsd1, Vpsd1 TAsd2, AAsd2, Vpsd2
If |TAm2 –TAm1| > TAsd1 and TAsd2, then it will be possible to estimate the entry velocity, since at short distances (below 100 km), |Vpm2 – Vpm1| is proportional to the height difference between both subsets.

If |AAm2 –AAm1| > AAsd1 and AAsd2, and if significant data from at least one more array are available, it will be possible to estimate the direction of entry.
The difference |Vpm2 – Vpm1| may be converted into the difference of angles-of-incidence, Δe.

Table 6. Results of analysis for the Kiruna-array

Date	Rocket	|TAm2 –TAm1| seconds	Δe degrees	Δe /|TAm2 –TAm1| deg/sec	ΔAz degrees
1998-11-24	Castor 4E	22.3	3.45	0.155	0.5
2001-04-29	"	35.6	7.97	0.224	0.9
2003-04-01	"	12.3	4.48	0.364	2.7
2004-11-22	"	22.3	3.79	0.170	6.1
2005-05-02	"	11.1	6.96	0.626	0.3
2004-12-02	Skylark 7	18.0	2.35	0.131	3.8
2005-12-01	"	0.9	0.23	0.256	~0
2006-05-11	"	14.3	1.47	0.103	1.9

Due to the small number of cases, it is not meaningful to calculate averages for each rocket. However, it can be seen that the speed of change of the angle-of-incidence is larger for the larger rocket, Castor 4E. This observation is consistent with the fact that Castor 4E has a significantly greater entry velocity than Skylark 7 (see Table 2).

At the Jämtön-array, 319 km from the impact, not all rocket launchings were recorded, as can be seen from Figs. 3 – 10. In one case, although the signal was recorded, no significant results could be obtained due to propagation effects. The results of analysis are shown in Table 7.

Table 7. Results of analysis for Jämtön-array

Date	Rocket	|TAm2 –TAm1| seconds	Δe degrees	Δe /|TAm2 –TAm1| deg/sec	ΔAz degrees
1998-11-24	Castor 4E	No signal	-	-	-
2001-04-29	"	11.1	2.42	0.219	0.4
2003-04-01	"	No signal	-	-	-
2004-11-22	"	28.9	4.75	0.164	2.8
2005-05-02	"	3.4	1.2	0.353	0.6
2004-12-02	Skylark 7	*)	-	-	-
2005-12-01	"	No signal	-	-	-
2006-05-11	"	58.3	6.66	0.114	*)

*) - No significant results

There is only one significant observation for Skylark 7, where the speed of change of the angle-of-incidence is also smaller than all those observed for Castor 4E.

The difference between the angle-of-arrival for both subsets, |AAm2 –AAm1|, denoted ΔAz, is shown in the last column of Tables 6 and 7. Since the entry of the rocket is nearly vertical, the observed ΔAz is a measure of lateral deviation of rays in horizontal gradients of wind and/or temperature. The present observations indicate that the orientation angle of the meteoroid's orbit, as determined from infrasonic observations, will be biased by propagation effects.

The above results will be applied to the analysis of a few close meteoroid impacts monitored by infrasonic arrays.

References to Chapter 3

Liszka L.: Propagation Effects and Localization of Infrasonic Sources, 1997, AGU Fall Meeting, San Francisco.
ReVelle D.O., W. Edwards and T. Sandoval: Genesis – An artificial, low velocity "meteor" fall and recovery: September 8, 2004. Meteoritics & Planetary Science 40, Nr 6, 819-839, 2005.

Chapter 4

Observations of Major Meteoroid Impacts by Infrasonic Arrays in Sweden

It has been shown by ReVelle (1997) that the dominating frequency of the infrasonic signal generated by a meteoroid entry is related to its total energy. However, the intensity pattern measured on the ground at different frequencies also carries information about the meteoroid's trajectory.

It has been shown (Procunier & Sharp, 1971) that the signal-to-noise ratio for acoustic waves generated at different heights varies with the altitude of the source, see Fig. 20.

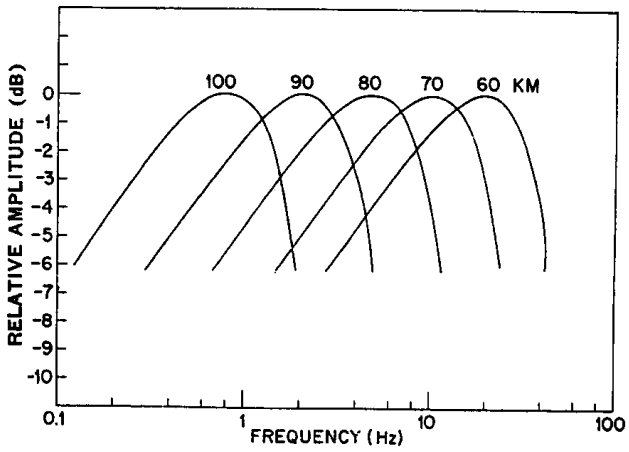

Fig.20. Signal-to-noise ratio for different source heights versus frequency (after Procunier & Sharp, 1971).

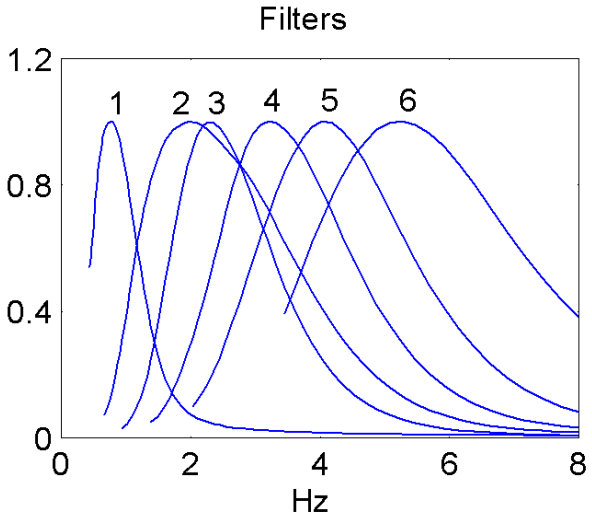

Fig. 21. Transmission curves for wavelet filters.

When the signal is viewed through a set of wavelet filters, like those shown in Fig. 21, the signal analysis at a given frequency will provide information about the angle-of-arrival and the horizontal trace velocity corresponding to a certain range of altitudes. In the case of a meteor impact, it may be expected that the variation of angle-of-arrival with frequency will

reflect not only effects of atmospheric winds, but also the orientation of the impact trajectory. It has been shown in an earlier section that in the case of nearly-vertical impacts of high altitude rockets, the lateral deviation of the ray as a function of frequency must be due to the atmospheric wind- and temperature profiles. In the case of meteoroid impacts, the angle-of-arrival will also vary with frequency if its trajectory has a tangential component across the line-of-sight.

The Jokkmokk-event

A spectacular meteor event occurred over northern Sweden on January 17, 2004, at approximately 1405 UT. The impact area was located about 50 km NW of the village of Jokkmokk, north of the Arctic Circle. During the days that followed, local newspapers reported a number of eyewitness observations of the event, despite the impact area being very sparsely populated. It was clear from all reports that what had happened on January 17 was a major event. Although it is almost completely dark at this time of the year in the meteor event region, the inhabitants of this area reported that at the time of the impact, the landscape was briefly illuminated as if it were full daylight. A number of loud explosions were also reported and there was apparently an eyewitness standing just below the bolide trajectory about 30 km NNE of the impact area.

The above description indicates that multiple fragmentations occurred at low altitudes, probably as low as 25 km.

Relevant data from all four arrays are presented in Fig. 22.

Fig.22. The Jokkmokk event

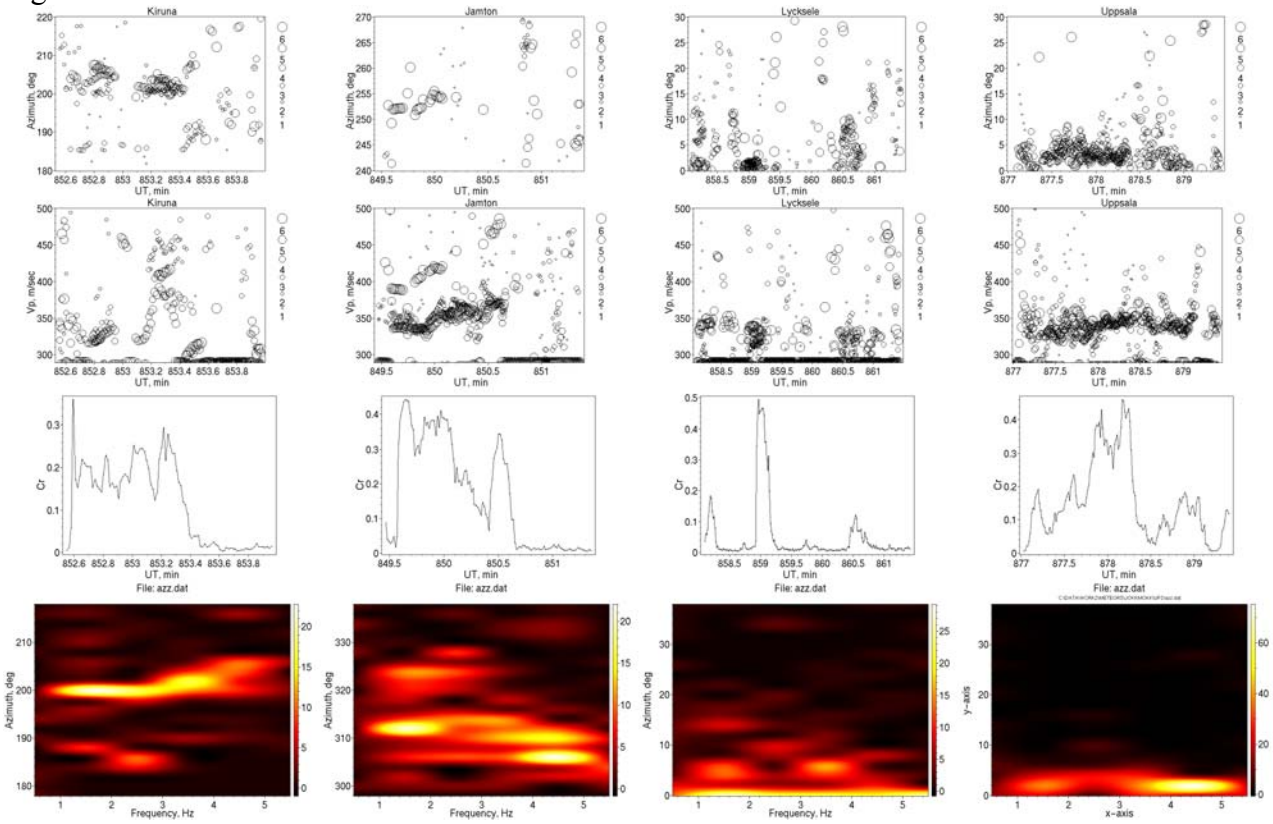

Sodankylä-radiosonde atmospheric data

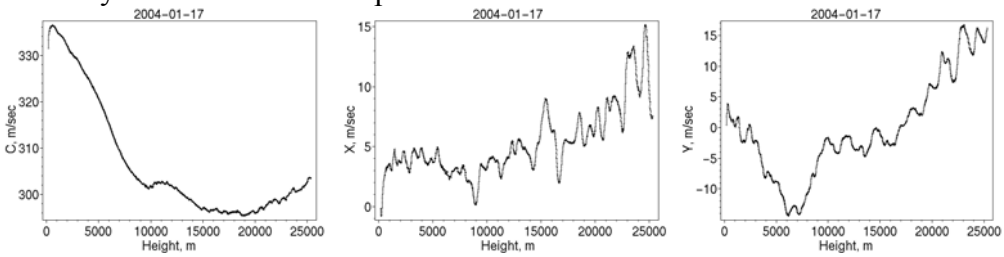

Fig. 22. The Jokkmokk event, 2004-01-17. Top row: angle-of-arrival, second row: horizontal trace velocity, third row: product of all three cross-correlations across the array. Fourth row: time-averaged histograms of the angle-of-arrival as a function of frequency. Arrays (from left to right): Kiruna, Jämtön, Lycksele, Uppsala. The bottom graphs: sound velocity (left), zonal (middle) and meridional (right) winds over northern Finland at noon (source: Finnish Meteorological Institute) up to an altitude of 25,000 m. Positive direction of the zonal wind is towards W, and of the meridional wind towards S.

The Bygdsiljum event

The event occurred on July 12, 2004 at 2116UT close to a village of Bygdsiljum, over the location 64.30N, 20.49E. It was observed and reported by many people in Finland and Sweden, on both sides of the Gulf of Bothnia. The event consisted of three explosions/fragmentations detected by the SIN stations. The infrasonic signal from the event was highly unisotropic (see Table 8).

Table 8

Station	Distance Km	Amplitude Max, Pa	Azimuth Deg	Frequency at max Hz	Phase velocity, m/sec
Kiruna	396	0.045	179	1.03	370-400
Jämtön	202	0.02	208	1.1	400
Lycksele	98	0.146	113	0.65	360-390
Uppsala	514	0.089	16	1.26	348

In Jamtön, the signal amplitude is at the detection limit, while in Uppsala, 514 km away, the signal amplitude is more than a half of its value at the closest station (Lycksele).
Relevant data from all four arrays are presented in Fig. 23.

The Tromsö event

The event occurred on June 7, 2006 at 0007 UT in Northern Norway (Finnmark). The meteor itself most probably exploded in the atmosphere at an approximate altitude of 10 to 20 km. The explosion was heard over a large area of northern Norway, and although the sky was quite bright due to the midnight sun, the event was also observed visually; pictures of its smoke trail were published in the daily newspaper *Aftenposten* on June 9, 2006.
The event was also detected by the ARCES seismic array in northern Norway (Schweitzer & Kværna, 2006).

All Swedish arrays recorded the event. However, in Kiruna, the signal was so strong that the equipment was completely saturated during a few minutes. Only the last, weakest, portion of the signal could be used for analysis.

Relevant data from all four arrays are presented in Fig. 24.

The Tromsö event is rather different from the previous two. It shows a striking, semi-regular modulation, visible from all stations, except for Kiruna. The modulation is most clearly seen on plots of the cross-correlation product (third row).

Bygdsiljum event

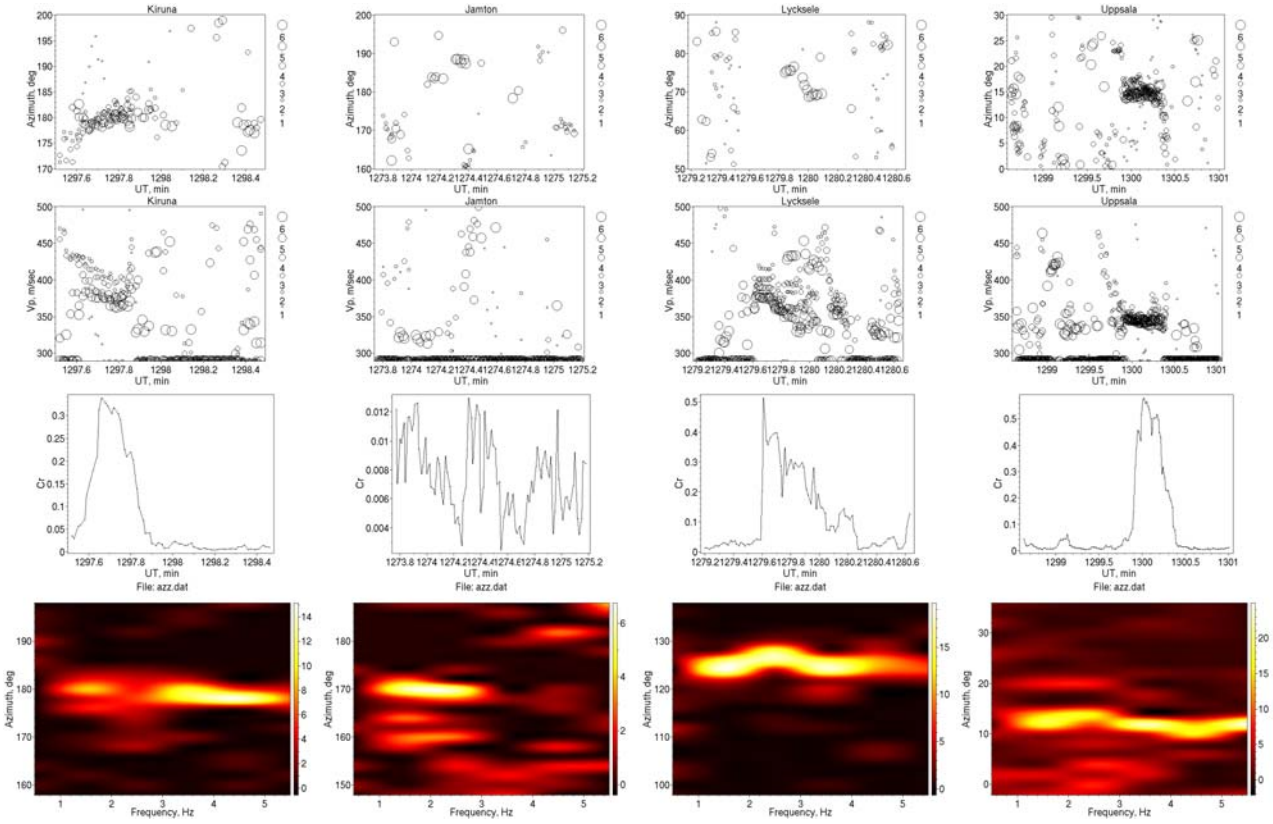

Sodankylä-radiosonde atmospheric data

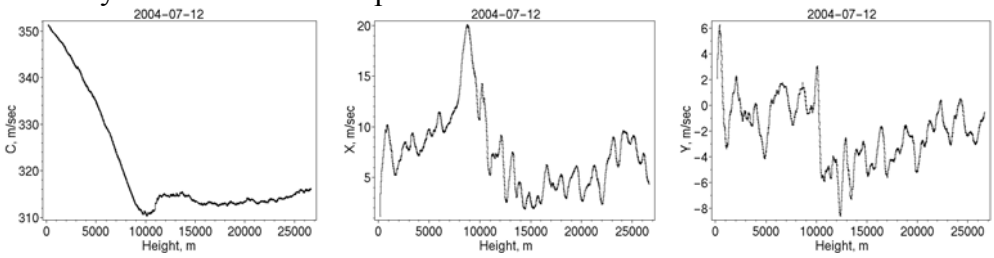

Fig. 23. Bygdsiljum event, 2004-07-12. Top row: angle-of-arrival, second row: horizontal trace velocity, third row: product of all three cross-correlations across the array. Fourth row: time-averaged histograms of the angle-of-arrival as a function of frequency. Arrays (from left to right): Kiruna, Jämtön, Lycksele, Uppsala. The bottom graphs: sound velocity (left), zonal (middle) and meridional (right) winds over northern Finland at midnight (source: Finnish Meteorological Institute) up to an altitude of 25,000 m. Positive direction of the zonal wind is towards W, and of the meridional wind towards S.

Tromsö event

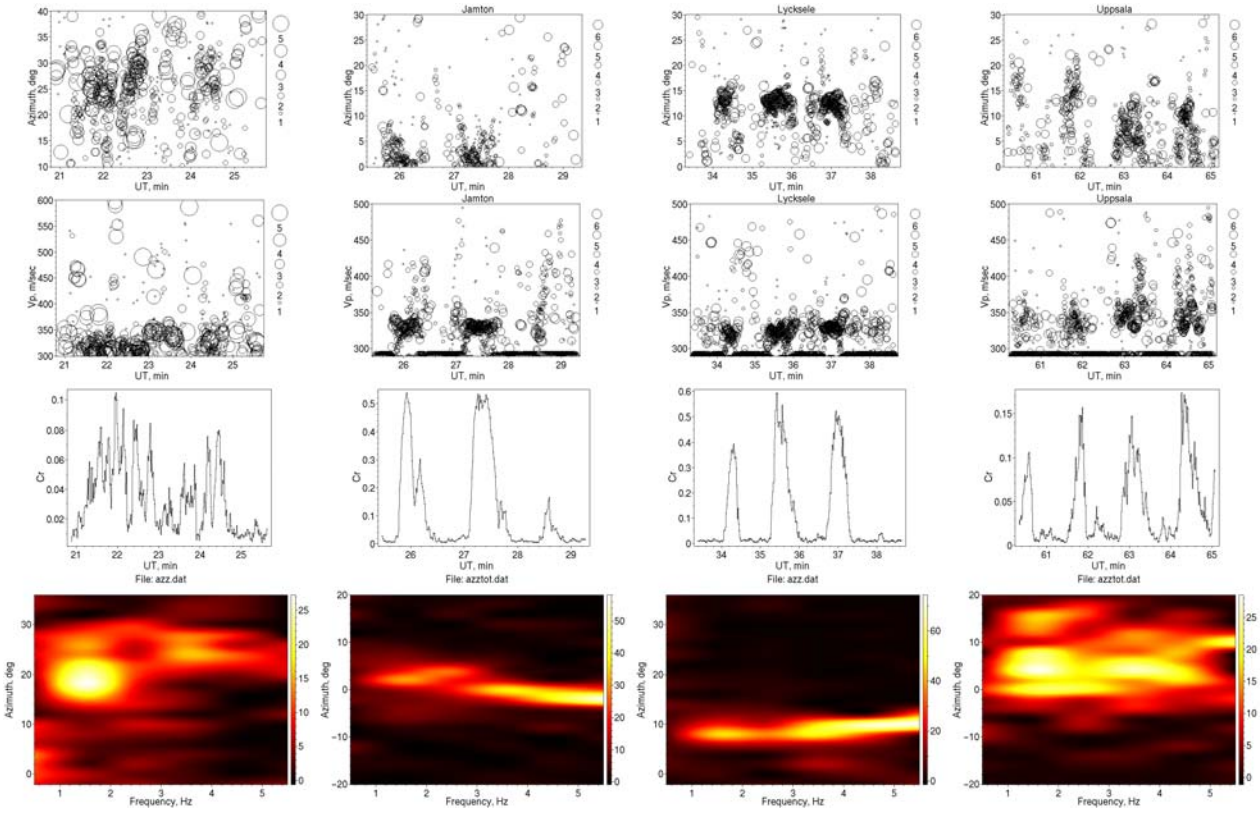

Sodankylä-radiosonde atmospheric data

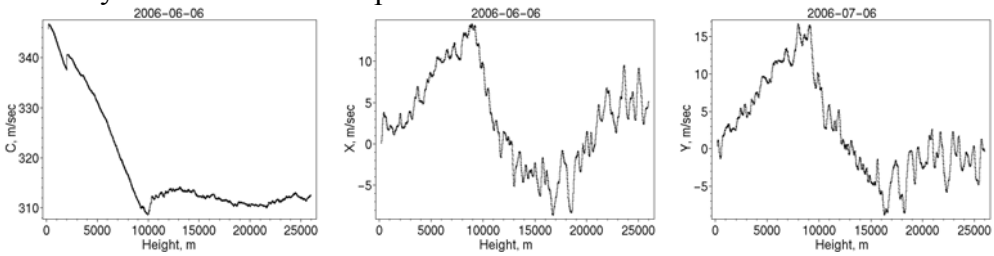

Fig. 24. Tromsö event, 2006-06-07. Top row: angle-of-arrival, second row: horizontal trace velocity, third row: product of all three cross-correlations across the array. Fourth row: time-averaged histograms of the angle-of-arrival as a function of frequency. Arrays (from left to right): Kiruna, Jämtön, Lycksele, Uppsala. The bottom graphs: sound velocity (left), zonal (middle) and meridional (right) winds over northern Finland at midnight (source: Finnish Meteorological Institute) up to an altitude of 25,000 m. Positive direction of the zonal wind is towards W, and of the meridional wind towards S.

Karelia event

Another unusual event was observed on May 17, 2005 across eastern Finland. The event was reported at the Global Meteor Observing Forum as an unusually bright bolide in the message reproduced below:

“

Date: Wed, 18 May 2005 15:56:47 +0300
From: "Lyytinen Esko" <Esko.Lyytinen@MINEDU.FI>
To: "Global Meteor Observing Forum"
Cc: marko.pekkola@ursa.fi
Subject: RE: Fireball News Article from Finland
Hi,
Yes we really had a very bright fireball yesterday evening at about 19.23 UT.
The URSA meteor section has received quite a big number of reports and more is coming. The Sun was just about setting at the region of the observations and it was very remarkable in spite of the lightness. It was cloudy here in Southern Finland and so I could not capture it in my fireball-camera.

We have received one photograph of the smoke trail that persisted for 45 minutes (maybe till the Sun got too low to illuminate it). There also exists a video of the smoke trail, but the recorder has not yet submitted it.

According to my quick lookup, this seems to be clearly visible in the Swedish infrasound data from http://www.umea.irf.se/maps/index.php Uppsala and Lycksele .
It appears to have entered from somewhere South-East with an entry angle of maybe 30 degrees from horizon and lasted maybe from 5 to 10 seconds. So the entry velocity seems to have been relatively slow. According to one (of the most nearby observers) it exploded into small pieced that ended in less than a second from the explosion.

The pieces quite clearly landed outside the Finnish border, into the Russian side, maybe by about/more than 100kms, according to the infrared locator. I expect that Markku Nissinen will put the smoke trail-figure into the URSA meteor section web-site, but this has not yet been done.
Esko

“

There are, as it is mentioned in the above message, high quality recordings of the event both in Lycksele and Uppsala. Therefore, it was possible to study the event in detail.

Karelia event

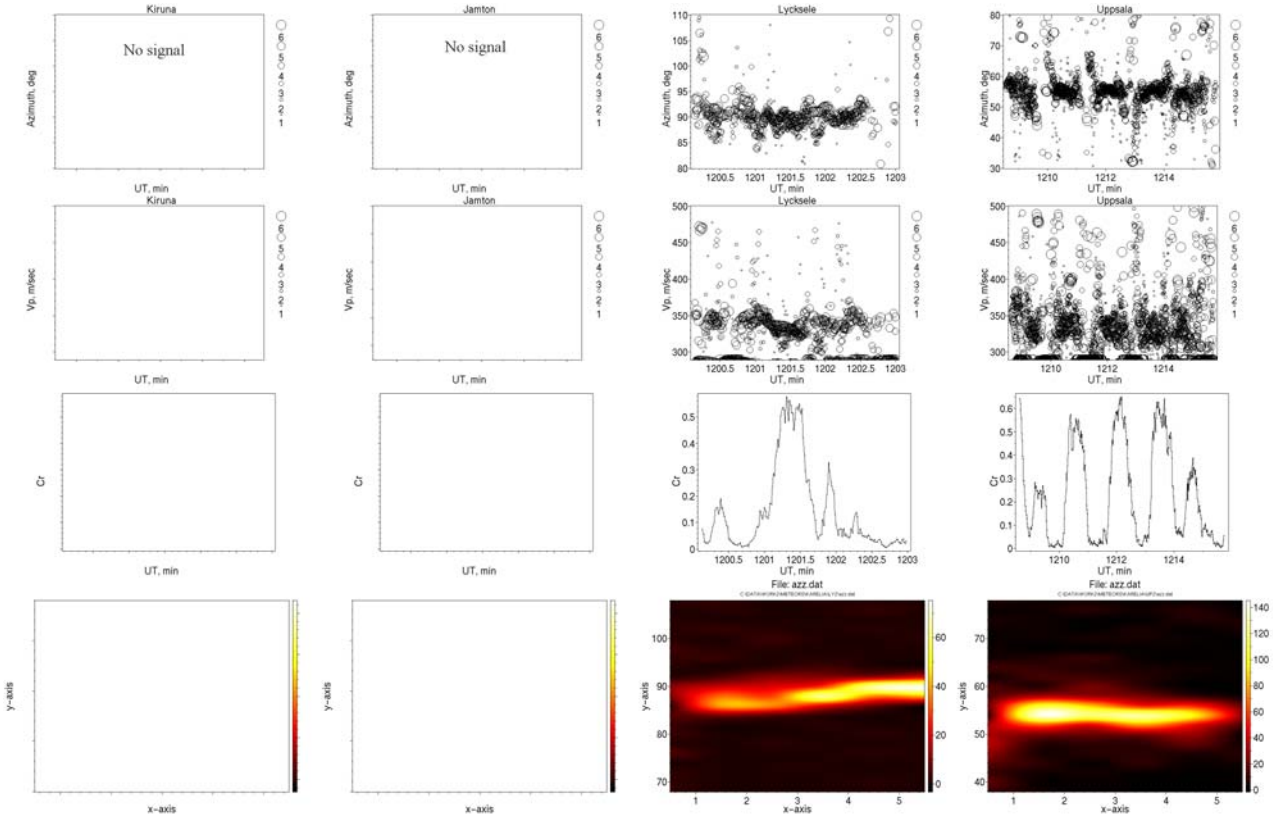

Sodankylä-radiosonde atmospheric data

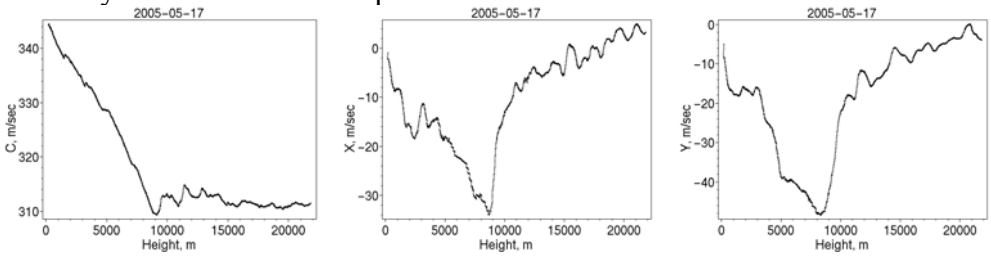

Fig. 25. Karelia event, 2005-05-17. Top row: angle-of-arrival, second row: horizontal trace velocity, third row: product of all three cross-correlations across the array. Fourth row: time-averaged histograms of the angle-of-arrival as a function of frequency. Arrays (from left to right): Lycksele, Uppsala. No signal detected at Kiruna- and Jämtön-array. The bottom graphs: sound velocity (left), zonal (middle) and meridional (right) winds over northern Finland at midnight (source: Finnish Meteorological Institute) up to an altitude of 25,000 m. Positive direction of the zonal wind is towards W, and of the meridional wind towards S.

However, there is no trace of detectable signals at the Kiruna- and Jämtön-arrays. There are some amazing circumstances about this event. In particular, when seen from Uppsala, the infrasonic signal is modulated (see the three upper graphs of Fig. 25) with a period of about 100 seconds. The modulation is also seen from Lycksele. There is a clear similarity to the Tromsö-event. Furthermore, reports about the trail persisting for 45 minutes are astonishing if this was a typical bolide. Using a method presented in a later section, the object's heading was calculated at a position 33.2E, 64.2N to be 320 degrees. The event detector, which will be described in a later section, applied to Lycksele-data, does not indicate any possible event at that time (Fig. 26).

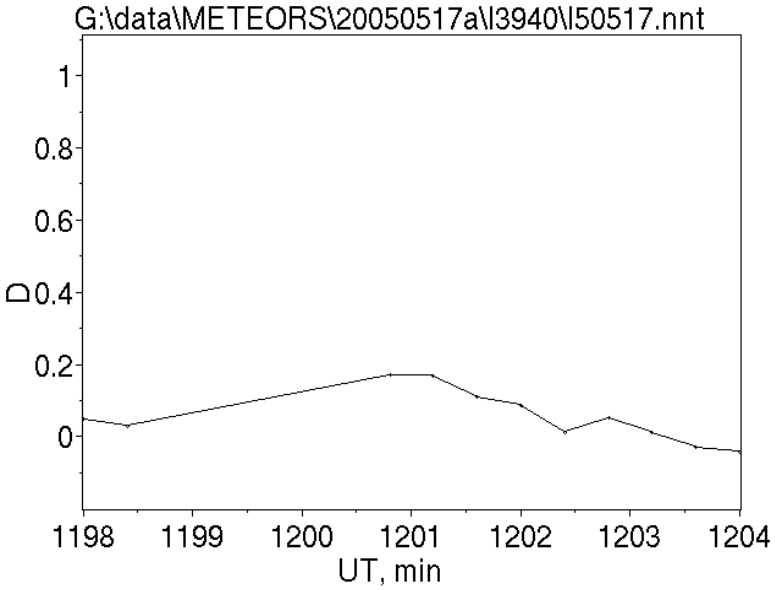

Fig. 26. The output of the event detector applied to Lycksele-data during the period covering the Karelia-event.

The Oulu event

Another major meteor event occurred in the evening of September 28, 2007 over a relatively dense populated area east of the Finnish town of Oulu. The event took place at 21:39 local time (18:39 UT), which explains the large number of witnesses across an area of several hundreds of kilometres. Finland's largest astronomical association, Ursa, informed that the light phenomenon seen over much of northern and eastern Finland on the night of September 28th was a meteor -- the brightest seen in the country in more than 30 years. The editor of the organization's journal (http://www.avaruus.fi/), Marko Pekkola, says it was a super-bolide, a fireball with a magnitude of –20, more than 100 times brighter than a full moon. According to Ursa, the fireball was apparently caused by a meteoroid striking the atmosphere over northern Ostrobothnia and then exploding over Finland. The rock may have weighed some 200 kg. However, it was not clear, at the time of the published article, whether any meteorites fell to the ground. The event spurred worried telephone calls to emergency centres in various parts of Finnish Lapland, as far apart as Kemi, Enontekiö and Ivalo.

Relevant data from three arrays, which were operated on that occasion, are presented in Fig. 27.

Oulu event

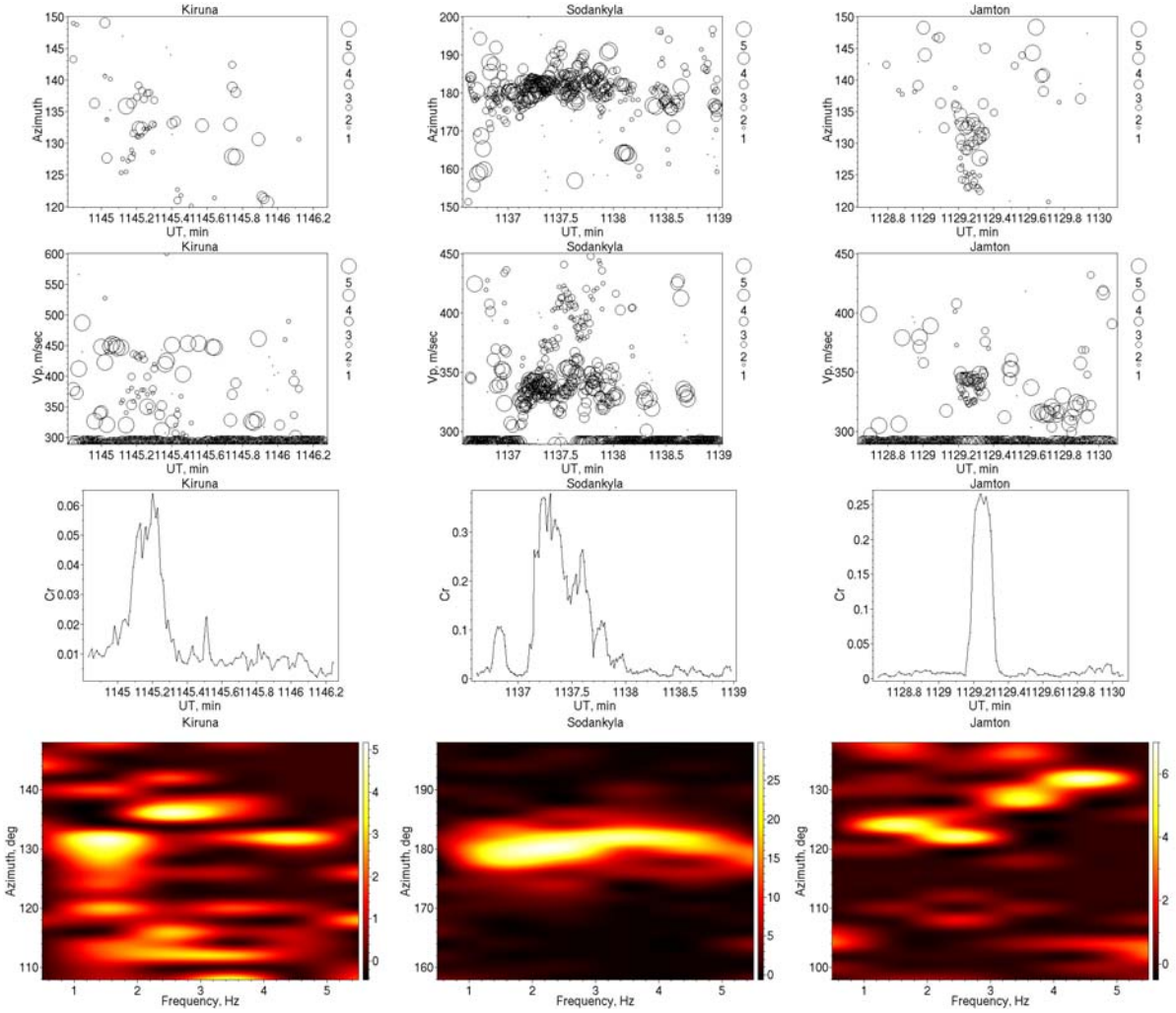

Sodankylä-radiosonde atmospheric data

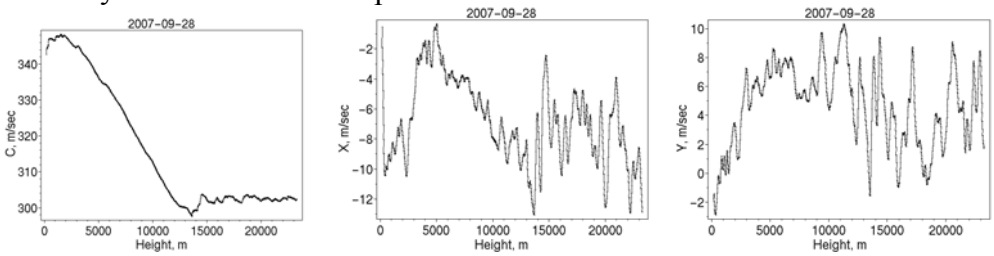

Fig. 27. Oulu event, 2007-09-28. Top row: angle-of-arrival, second row: horizontal trace velocity, third row: product of all three cross-correlations across the array. Fourth row: time-averaged histograms of the angle-of-arrival as a function of frequency. Arrays (from left to right): Kiruna, Sodankylä, Jämtön. Lycksele-array was not in operation at that occasion. The bottom graphs: sound velocity (left), zonal (middle) and meridional (right) winds over northern Finland at midnight (source: Finnish Meteorological Institute) up to an altitude of 25,000 m. Positive direction of the zonal wind is towards W, and of the meridional wind towards S.

Discussion of Results

The Karelia event

The distance between the event and both arrays where the event was detected is too large to be able to convert the trace velocity into the apparent elevation of the source. For this reason, only the horizontal location of the event could be calculated. The projection of trajectory segments obtained from the multi-frequency analysis is shown in Fig. 28.

Fig. 28. A horizontal projection of trajectory segments obtained from the multi-frequency analysis – Karelia-event.

The heading of the object was approximately 260 degrees. Since the projections of segments obtained for three frequencies overlap each other, it may be assumed that the entry trajectory was very steep, probably >70 degrees from the horizontal plane.

The Oulu event

A similar situation occurred in the case of the latest event, SE of Oulu, Finland. The closest array, Jämtön, is slightly more than 200 km from the object's trajectory. Observed trace velocities can therefore not be used as a measure of the object's elevation. Horizontal projections of trajectory segments, obtained from the multi-frequency analysis, are shown in Fig. 29. Data from all three arrays at Kiruna, Sodankylä and Jämtön are used to reconstruct the trajectory. It can be concluded that the object was heading nearly towards the south at a rather shallow angle.

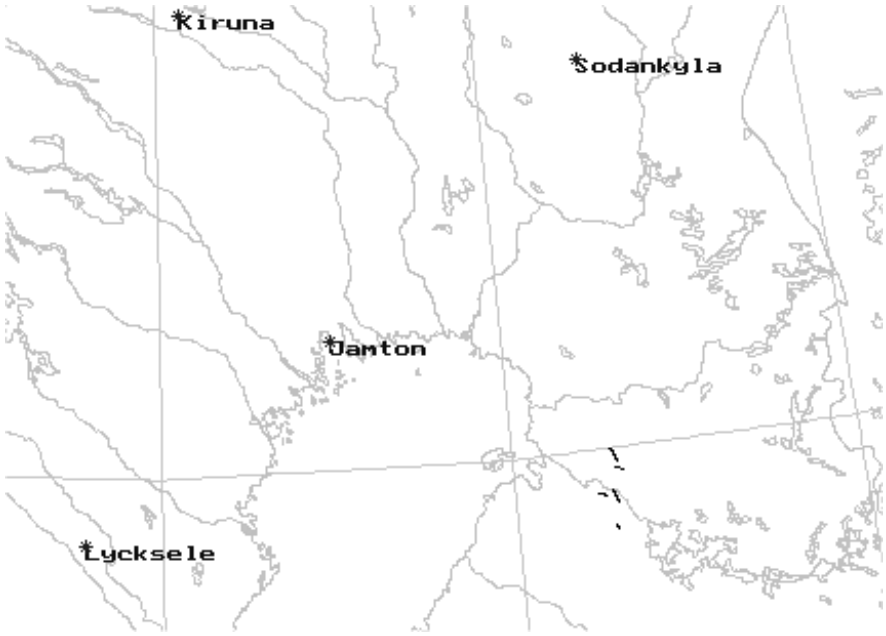

Fig. 29. A horizontal projection of trajectory segments obtained from the multi-frequency analysis and combining data from all three arrays – Oulu-event.

References to Chapter 4

Procunier R. W. and G. W. Sharp, J. Acoust. Soc. Am. 49, 622 (1971).

ReVelle, D. O.: 1997, Historical Detection of Atmospheric Impacts of Large Bolides Using Acoustic-Gravity Waves, Ann. NY Acad. Sci., in J. L. Remo (ed.), Near-Earth Objects- The United Nations International Conference, The New York Academy of Sciences, New York, New York, Vol. 822, pp. 284–302

Schweitzer, J. & T. Kværna (2006): Infrasound observations of two recent meteor impacts in Norway. **In:** Semiannual Technical Summary, 1 January - 30 June 2006, NORSAR Sci. Rep. 2-2006, Kjeller, Norway.

Chapter 5

Extraction of Orbital Information from Infrasonic Observations

Localization of Infrasonic Sources

A single tripartite array provides measurements of the angle-of-arrival and of the horizontal trace velocity across the array. The method for determination of those variables was described by Waldemark (1994). The trace velocity is related to the inclination angle of the wave vector. For nearby sources, the inclination angle is close to the apparent position of the source. For distant sources it is also controlled by conditions along the propagation path. For supersonic sources, it is also dependent on the velocity of the source. Single array measurements do not provide any clear information about the distance to the source. In order to determine the distance to the source, a pair of microphone arrays, spaced at a long enough distance, is needed. In a two-dimensional plane case, the problem is very simple (Fig. 30). On the Earth's surface, however, especially when large distances are involved, even a spherical solution is not good enough, thus the problem must be solved on a geoid. Software for different assumed geoid models may be downloaded from the same Internet site as the other software previously mentioned. The software **locmod.exe** determines the position X for given angles A_1 and A_2 and a specified pair of stations. The software **arrival.exe** calculates times of arrival of the signal at all SIN stations for a given geographic position of X and the time of origin of the signal.

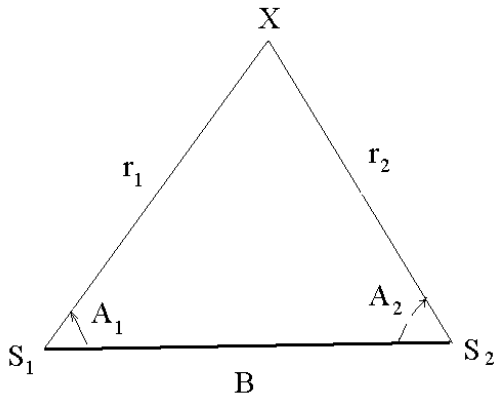

Fig. 30. Determination of distance from two microphone arrays, S_1 and S_2

The accuracy, with which the source position may be determined, depends on the distance between arrays, B, and on both the values of angles A_1, A_2 and on their accuracy. The error in the determined distance r_1 or r_2, Δr may be estimated as:

$$\Delta r = |\partial r/\partial A_1| * \Delta A_1 + |\partial r/\partial A_2| * \Delta A_2 \qquad (2)$$

where ΔA_1 and ΔA_2 are errors in the angle–of-arrival measured at both arrays (approx. 1 degree). On the geoid, the localization accuracy depends also on geographical coordinates of both arrays. Both derivatives of equation (2) may be computed numerically for given geographical locations of arrays and a given combination of angles-of-arrival. It is obvious that the localization has the lowest accuracy when the source is located close to the direction of baseline B. The accuracy problem may be illustrated as follows: For a given pair of arrays, we assume a source at a variable location, but fulfilling a condition that the difference

between 180-A_1 and A2 is constant, for example, 5 degrees. The location of the source may be calculated as a function of any pair of A1 and A2 using the software locmod.exe.

Furthermore, partial derivatives of eq. (2) may be calculated numerically. Thus, the localization accuracy will be determined with respect to the orientation of the baseline. The results of computations for pairs of arrays: Kiruna-Jamton and Jamton-Lycksele are shown in Fig. 31.

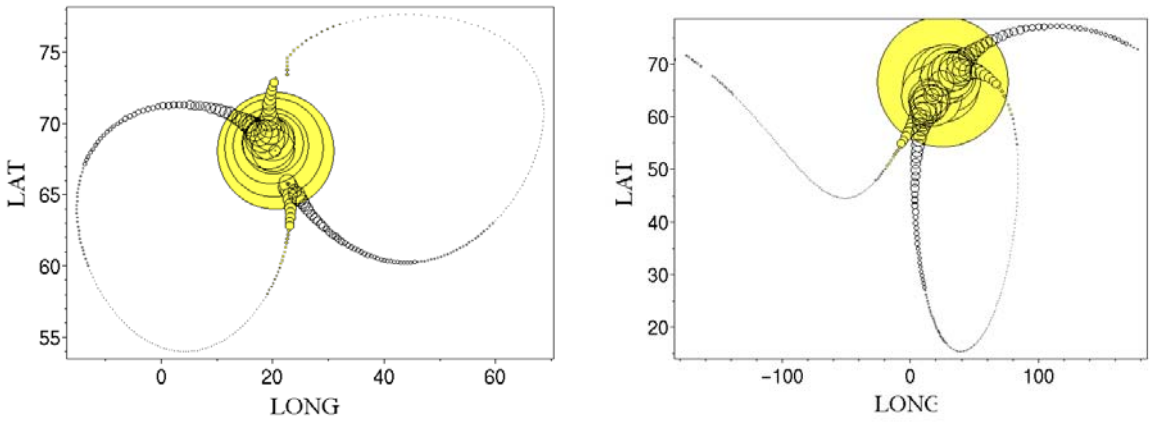

Fig. 31. Relative localization errors for array pairs: Kiruna-Jamton (left graph - baseline direction 179 deg.) and Jamton-Lycksele (right graph – baseline direction 234.7 deg.)

Localized positions are shown by circles with diameters proportional to the relative accuracy of distance determination. The smallest circles plotted correspond to 2% errors in the distance. It is apparent that close to the baseline direction, the source localization is undetermined (relative errors > 100%). The conclusion is that different combinations of arrays must be used for localization in different geographic areas.

Moving Sources: Subsonic and Supersonic

When observing close stationary sources, the sequence of recorded infrasonic signals is the same as at the source. Localization of close stationary sources is straightforward and requires only a simple statistical signal analysis. Of course, for distant sources, the situation is more complicated since the multi-path propagation mixes together signals originated at different instants.

For subsonic sources, moving at short distances, the signal sequence has to be corrected for the varying propagation time before data from two arrays can be matched together, so that the right pairs of angle-of-arrival from different arrays are used for localization. The order of the observed signal sequence is, however, the same at both arrays and at the source, especially when the source is not too close to the baseline between the arrays.

For supersonic sources, the observed signal sequence may be either the same as at the source, or reversed. It makes matching of angle-of-arrival from different arrays difficult. Furthermore, both arrays may see different parts of the source trajectory.

In the simplest case, there is the same order of events at both arrays, i.e. the signal start is seen first at both locations. Then it is still unknown which points of the signal correspond to each other. Fixing the starting point of signal at the array 1, the matching point of the signal at the array 2 may be varied by one data point at the time, thus a number of possible source trajectory will be obtained. That procedure may be repeated for different combinations of arrays. A mass plot of possible trajectories will be obtained (see Fig. 32).

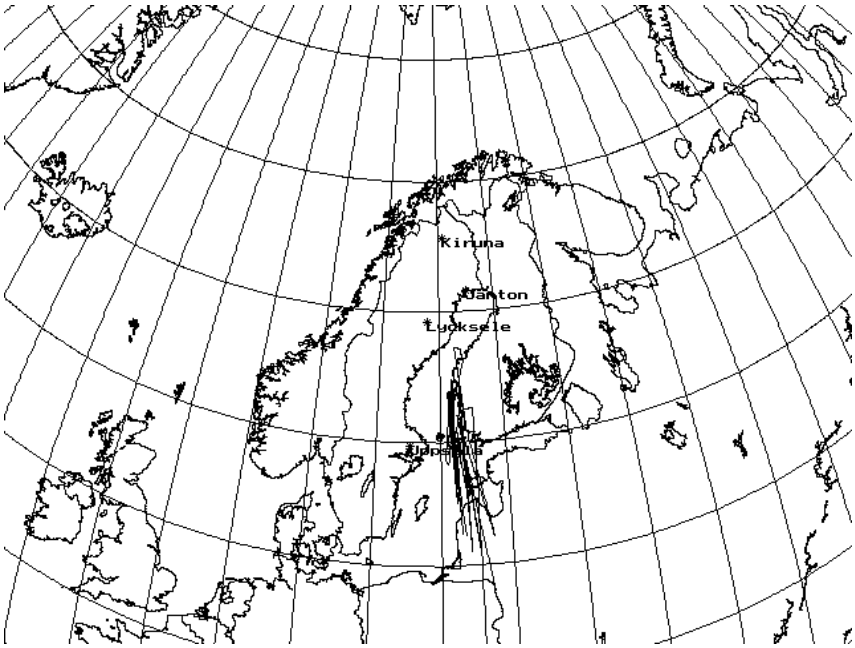

Fig. 32. A plot of possible trajectories of a supersonic object on January 18, 2006 at 17:40 UT.

The real trajectory is probably located in the region of largest density of possible trajectories. The event of Fig. 32 is most likely a supersonic aircraft flying northward over a large horizontal distance at approximately Mach 1.5.

When observing supersonic sources it often happens that the observed order of events is different at different arrays. The start of the infrasound-generating trajectory may arrive first at one station, but it may arrive last at another station. It may be due to both the geometry of the trajectory and the source speed, but also due to effects of the atmospheric wind system and atmospheric irregularities, as was shown in Chapter 3. If during the acoustically active trajectory the source of either the speed or the altitude (or both) varies, the problem may be solved using the measured trace velocity. The following procedure may be used;

- The sequence of computed data describing the signal (time-of-arrival, T, angle-of-arrival, A, and trace velocity, V) are sorted with respect to the trace velocity and three outermost outliers on each side of the distribution are removed.
- The distribution is divided into two equal parts, low, L, and high, H, one on each side of the median value.
- New median values are calculated for all three variables and for both partial distributions:

T_{L1}, A_{L1}, V_{L1} and T_{H1}, A_{H1}, V_{H1}. A_{L1} and A_{H1} are the lower and upper quartiles of the original distribution, respective.

- The same procedure is repeated for the same event data recorded at another array and a new set of values: T_{L2}, A_{L2}, V_{L2} and T_{H2}, A_{H2}, V_{H2} is obtained.

The medians have to be validated as described in Chapter 3.

The procedure marks two points, P_1 and P_2, on the acoustic active part of the source trajectory as seen at both locations. If there is a significant variation in the trace velocity, V, at both arrays, the order of events may be determined. For a meteoroid entry, the event will start with a high trace velocity (highest speed and altitude). Observations from both arrays may now be matched together, assuming that marked points with high trace velocity, P_1, correspond to the upper part of the trajectory. In the same way, points with lower trace velocity, P_2, will be attributed to the lower part of the trajectory. The present procedure may be useful when extracting orbital information from the data.

Extraction of the Orbital Information

It has been found that for events up to 100 km, until propagation effects will dominate the signal properties, it is possible to obtain certain orbital information from the data, in particular, when the recorded signal is generated by fragmentations (point sources). The main difficulty is that wind and temperature profiles between the source and the observer are not known in detail. The atmospheric variability is so great, that the use of temperature- and wind models barely improves the result of localization. In particular, in order to convert the observed trace velocity into the inclination of the wave vector, the real temperature and wind distribution in the atmosphere must be known. For this reason, for events farther away than 100 km from both arrays, only the horizontal projection of trajectory between points P_1 and P_2 may be determined applying the standard locmod-function to angles-of-arrival from two arrays. Geographical locations of points and the propagation times to both arrays are obtained as an output. Since the points P_1 and P_2 are usually relatively close to each other, spherical trigonometry formulas may be used to calculate the horizontal distance between the points, and the orientation angle of the line between the points with respect to the geographical North. Correcting the median times at both points by propagation times to both arrays, a velocity estimate (its horizontal component) can be made. The use of median times introduces an uncertainty here, since in the distribution of angles-of-arrival, event points in the same bin have very different times of arrival due to propagation effects.

For close events, assuming that trace velocities at points P_1 and P_2 as seen from at least one array, may be converted into the inclination of flight trajectory, an estimate of the entry angle can also be obtained.

Orbital Information from Three Close Events

The procedures described in earlier sections were used to estimate orbital elements for three major, close meteoroid entries:

The Jokkmokk event

Applying the earlier described procedure, coordinates of quartile points P_1 and P_2 calculated at different frequencies are shown in Table 9 for these two arrays (Kiruna & Jämtön), which were most favourably located with respect to the impact area.

The Kiruna-array was closest to the impact area (< 100 km) where the clear dependence between the trace velocity and wave frequency was found (see Fig. 33). The trace velocity is converted there into the ray inclination.

Table 9. Jokkmokk-event (as recorded at the Kiruna- and Jämtön-array)

Frequency Hz	P1 Long	P1 Lat	P2 Long	P2 Lat	H1 km	H2 km	Heading Deg
2.5	19.53E	67.21N	19.75E	67.48N	43.9	49.6	198
3.5	19.28E	67.15N	19.51E	67.27N	26.1	49.0	216
4.5	19.27E	67.08N	19.29E	67.16N	25.2	40.6	188

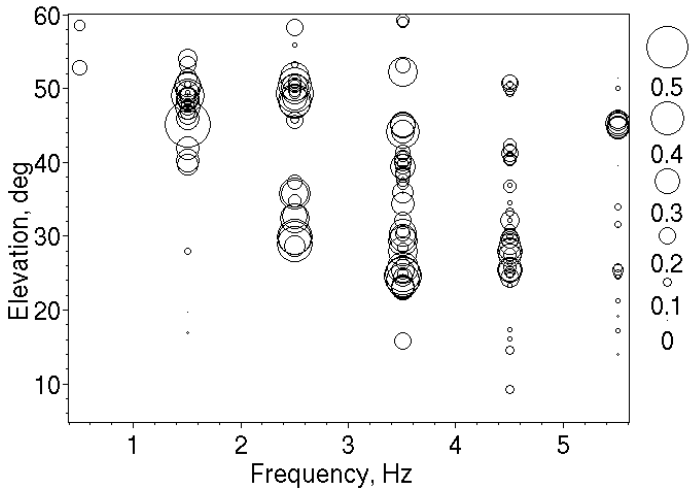

Fig. 33. Ray inclination for Jokkmokk event, seen from Kiruna, as a function of frequency. The size of the symbols is proportional to the product of all three cross-correlations across the array.

At 3.5 Hz, where the highest significance is obtained, locations imply a heading of the trajectory of 216°, measured from geographic North. It also corresponds to a horizontal distance between quartile points of 31.5 km. The slope of trajectory is estimated to 36 degrees. The estimated trajectory segments from Table 9 are plotted for all three frequencies on a 3-D graph (Fig. 34). Differences between segments, as seen at different frequencies, are due to the fact that they correspond to different height intervals and are influenced in different ways by the atmospheric conditions.

As shown in Fig. 34, the signal, recorded at Kiruna, indicates the occurrence of 3-4 fragmentations. Therefore, the median times-of-arrival cannot be used for determination of the entry velocity. A rough estimate indicates that the entry velocity was low, probably on the order of 8 km/sec.

This speed estimate is very low for a meteoroid entry and would rather agree with a space debris re-entry.

There is, in fact, on that day a re-entry report from the Aerospace Corporation (http://www.reentrynews.com/past.html) that could possibly be related to the Jokkmokk-event (see Fig. 35). According to the predictions, the re-entry was expected to take place well NW of Scandinavia. However, it cannot explain the Jokkmokk-event.

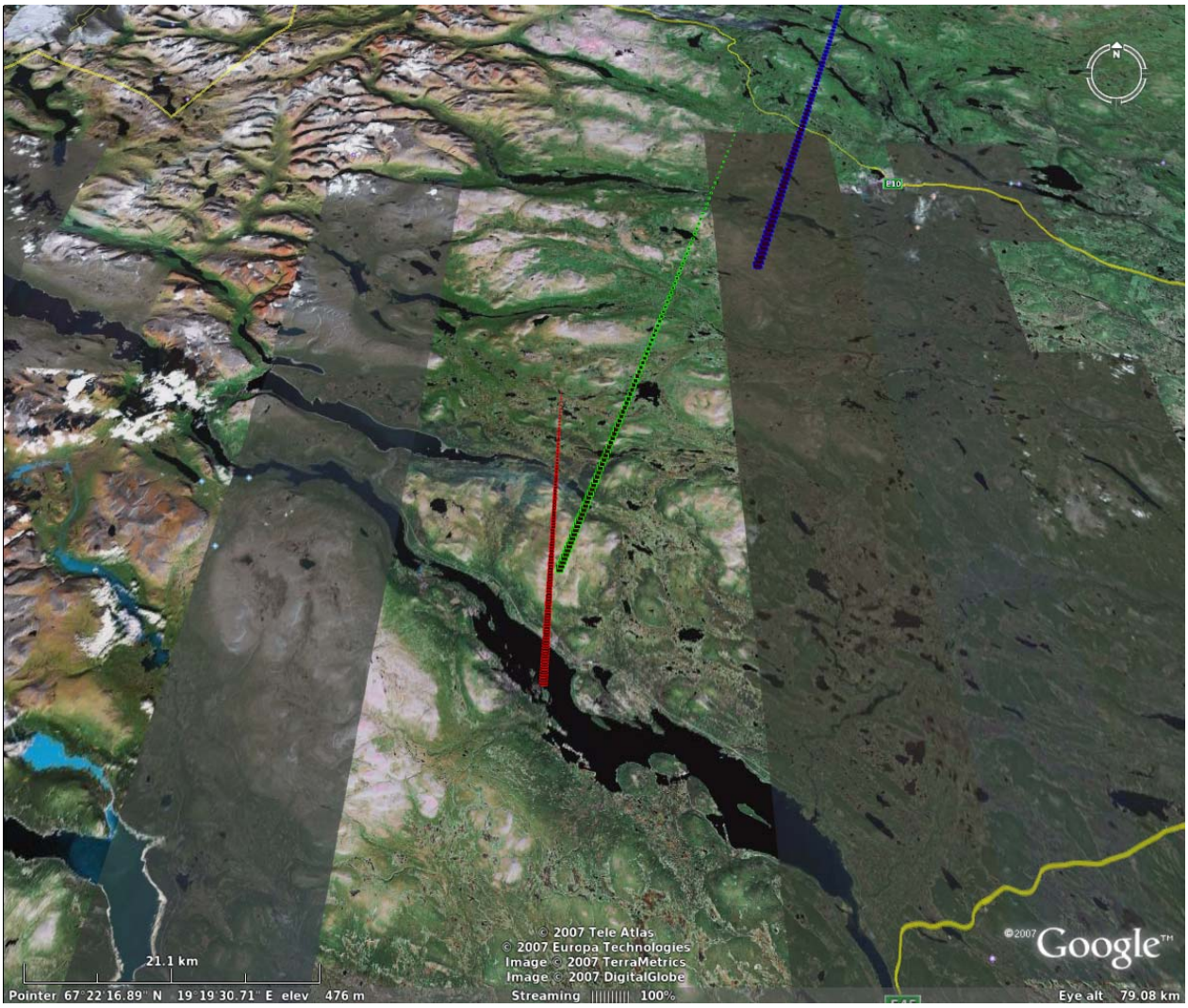

Fig. 34. Segments of the meteoroid trajectory, as seen at 2-5 (blue), 3.5 (green) and 4.5 Hz (red) plotted in 3-D above northern Sweden (source of the satellite image: Google Earth).

Object Description:

Type:	Start-1 Stage 4 Rocket Body
NORAD Name:	SL-18 R/B
NORAD Number:	26632
Int'l Designation:	2000 079B
Launched:	05 DEC 2000
Site:	Svododniy Cosmodrome LC5
Mission:	Ofeq 3

Reentry Prediction:

Predicted Reentry Time:	17 JAN 2004 @ 12:14 UTC ± 30 minutes
Prediction Epoch:	17 JAN 2004 @ 10:43:42.474 UTC

Prediction Ground Track:

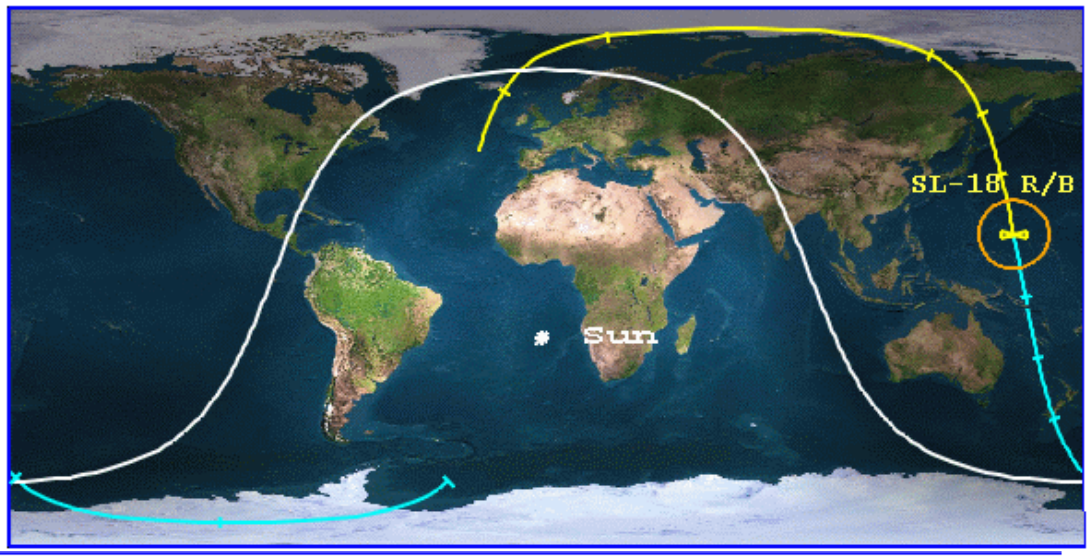

Ground track plotted at 5-minute intervals
Blue Line - ground track uncertainty prior to predicted time
Yellow Line - ground track uncertainty after predicted time
Orange Line - Earth horizon as seen from the reentering body
White Line - day/night terminator (Sun location as indicated)

USSTRATCOM Bulletin:
(from NASA/GSFC Orbital Information Group)

```
PREPARATION DATE TIME:  171553ZJAN04
1.  26632/2000-079B   /SL-18 R/B              /ROCKET BODY/ CIS
2.  05 DEC 2000
3.  REV  17596/DESCENDING/17 JAN 1311Z
4.  56.4 DEG S   314.8 DEG E
5.  DECAY WINDOW IS PLUS OR MINUS    01 HOURS.
6.  INCLINATION  097.1 DEGREES.
TRAJECTORY PRIOR TO DECAY (DEG):
D/TIME 017/1156Z    017/1211Z    017/1226Z    017/1241Z    017/1256Z
LAT.      -57.0          4.5         65.8         50.8        -11.1
E LONG    174.4        159.0        139.8        340.8        326.9
7.  FINAL REPORT.
```

Fig. 35. A debris re-entry report from the Aerospace Corporation regarding an event on January 17, 2004.

The Bygdsiljum event

Applying the quartile point analysis, P_1 and P_2 will be located at different geographic positions, depending on the frequency of observation:

Table 10. Bygdsiljum-event (as recorded at the Kiruna- and Lycksele-array)

Frequency Hz	P1 Long	P1 Lat	P2 Long	P2 Lat	H1 km	H2 km	Heading Deg
2.5	20.51E	64.26N	20.79E	64.18N	46.6	70.9	303
3.5	20.60E	64.28N	20.59E	64.27N	35.0	46.1	213
4.5	20.56E	64.26N	20.62E	64.28N	17.0	36.5	237

Only the heading determined for 2.5 Hz agrees with visual observations. However, the analysis results in unreasonably low computed horizontal speeds. A detailed, manual study of the event indicates that it may consist of two independent entries within a time interval of approx. 3 seconds. The first object undergoes a fragmentation, which explains 3 observed explosions. Matching the explosions recorded at both arrays, the coordinates E_1, E_2 & E_3 are obtained:

E_1 (20.5937E 64.2814N),
E_2 (20.5629E 64.275N),
E_3 (20.5067E 64.2615N),

where E_2 seems to be an independent event. Only E_1 and E_3 may therefore be used to determine the horizontal speed and the direction of motion. The horizontal speed between E_1 and E is estimated to 2.8 km/sec. Using the measured trace velocities from the closest station as a measure of the apparent height of the source, the inclination angle of the trajectory is estimated to 73.5°. Using the determined horizontal speed and the inclination angle, the total speed at the final part of the entry may be estimated to approximately 10 km/sec. The estimated inclination angle is in good agreement with optical images of the event taken on both sides of the Gulf of Bothnia.

The Tromsö event

Applying the quartile point analysis to this event, it is necessary to remember that the closest array (Kiruna) recorded only the final part of the signal. Combining data from Kiruna- and Jämtön-arrays, obtained at different frequencies, the entry trajectory of Fig 34 is obtained.

Fig. 36. The horizontal projection of trajectory segments determined at different frequencies (from N: 2.5, 3.5 and 4.5 Hz) combining Kiruna and Jämtön data.

Fig. 37. A 3-D presentation of trajectory segments shown in Fig. 35.

Reference to Chapter 5

Waldemark, K., (1994). High Resolution Infrasonic Recording Equipment, Scientific Rep., Swedish Institute of Space Physics.

Chapter 6

A Method for Automatic Recognition of Signals from Meteor Events

Description of Signals Using the Multiple Indicator Method

Indicators are distributions of variables within a given analyzing window:

- **Angle-of-arrival:** a distribution of angle-of-arrival is constructed using 10-degree bins. Then the distribution's entropy is calculated. The entropy value is used as one indicator.
- **Horizontal trace velocity:** a distribution is constructed using 50 m/sec bins. The distribution counts between 300 and 700 m/sec are used as indicators (8 values).
- **Cross-correlation across the array:** a distribution is constructed using 0.1 bins. The distribution counts between 0.15 and 0.85 are used as indicators (7 values)
- **Spectral slope:** the average spectral slope (in A/D units per Hz) of FFT spectrum between 0.4 and 1 Hz. The slope is mostly determined by the high-pass filter of the microphone, but is also influenced b y the shape of the low frequency part of the spectrum. A distribution is constructed using 1000 A/D unit bins. The distribution counts between 0 and 6000 are used as indicators (6 values).

On a total, the signal is described by a vector of 22 indicators (1 + 8 + 7 + 6).

Reference Events

The next step of the analysis is to establish a set of reference data which will be used to calibrate the method. The following major events will be used (Table 2):

Table 2

Date	Location
2001-10-27	North Sea
2002-04-02	Bavaria
2004-01-17	Jokkmokk, Sweden
2004-07-12	Bygdsiljum, Sweden
2005-02-05	North Sea

Multiple indicator vectors are calculated for the above events including +/- 10 minutes of signal-free background on both sides of each event. A 23rd column is added to the multiple indicator vectors: 0 in the absence of the signal and 1 in the presence of the signal. The reference data are then used to train a neural network model.

The Neural Network Model

It has been found that a back-propagation type of neural networks is adequate enough to model properties of the meteor entry signal. The development software NW2v530 was used. The network configuration used here is shown in Fig. 38.

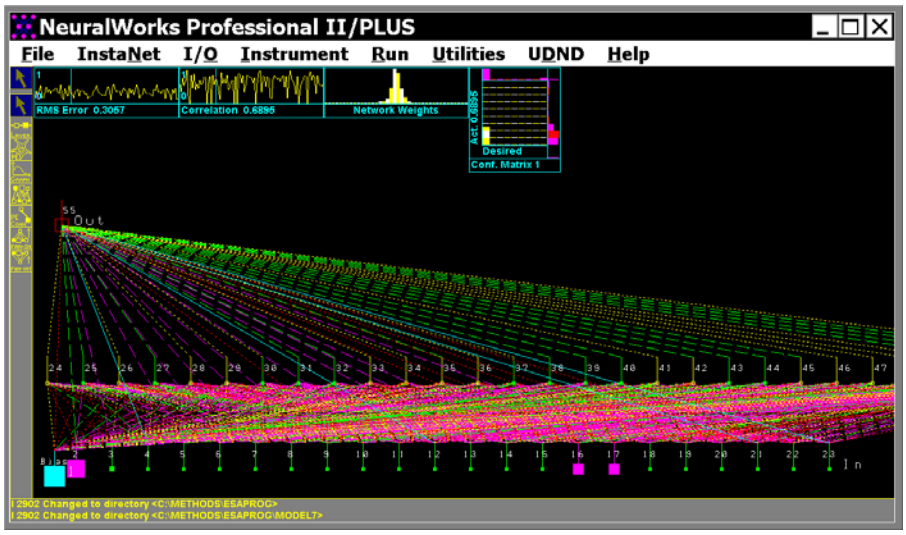

Fig. 38. The back-propagation type neural network used to develop a model of infrasonic signals from meteoroid entry events. The network has 22 input elements, 31 elements in the hidden layer and one element in the output layer.

During the training phase, 22 components of the multiple-indicator vector are placed in the input and the corresponding 23rd value (0 or 1) is placed in the output. The operation is repeated randomly 500,000 times until the network weights and hidden layer elements approach stable values. Training of the network is assumed be completed and it may be used in the recall mode. In this mode, arbitrary values of the 22-component vector are placed in the input. The network then calculates the corresponding output. If the vector is similar to those recorded during an entry event, an output close to 1 will be obtained. If the output is close to 0, the analyzed signal does not show any similarity with the reference entry events. The ready model is extracted in a format of so-called flash-code, which may be converted into an .exe-file. The model, an event detector, generates a single output for each given value of the 22-component vector.

"Confirmed Events"

Unfortunately, there is often no absolute proof that the detected event is really a meteoroid entry. Even a testimony of visual observers may sometimes be incorrect. A best example is the Karelia event of 2005-05-17. The event was reported at the Global Meteor Observing Forum as an unusually bright bolide (see Chapter 4). The absolute proof may be obtained only when fragments of the meteoroid are found, which is seldom.

Data Screening Procedure

Since the number of recorded signals per day may be large, it is practically impossible to study in detail all recorded signals in order to decide whether a given signal may be due to a meteoroid entry. In addition, the screening of complete data from all stations would be a very tedious project. Here, only Lycksele data were studied in detail and other stations were used only in cases when a possible event was found in Lycksele. The Lycksele station has a lowest background level and the best average coverage over the past 10 years. An important part of

the screening procedure is to correlate the output of the event detector with significant infrasonic signals.

The data analysis software, crcorr.exe, produces a large amount of values of angle-of-arrival and trace velocity, which must be statistically validated. One possibility is to apply a sliding window within which one value of weighted average will be calculated for both variables. A frequently used weighting factor is the cross-correlation across the array. However, it has been found that the best results are obtained weighting both variables with a factor $1/|A_i - A_{i+1}|$ (inverted differences between adjacent readings of the angle-of-arrival). A similar weighting method is used when following moving targets with radar.

An example of a daily plot showing validated infrasonic signals is given in Fig. 39. The angle-of-arrival for each signal is plotted as a circle, whose diameter is proportional to the average weighting factor.

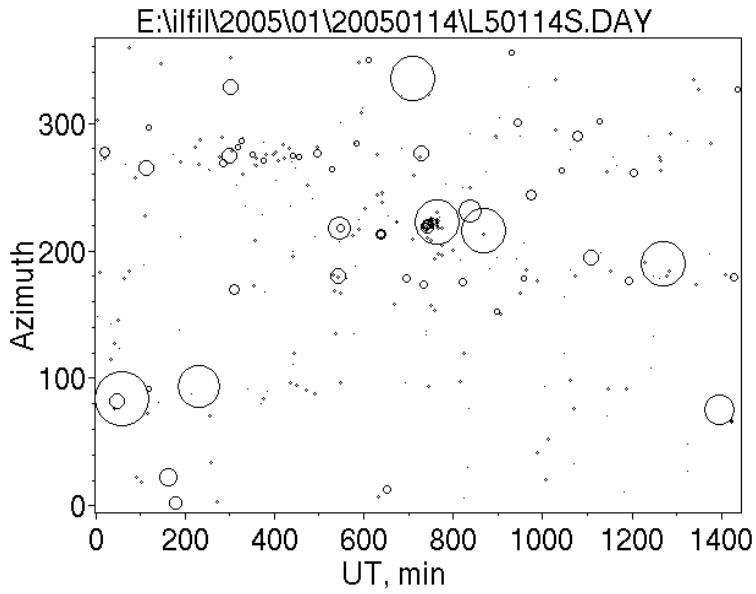

Fig. 39. An example of a daily plot showing validated infrasonic signals. The angle-of-arrival for each signal is plotted as a circle, whose diameter is proportional to the average weighting factor.

When applying the event detector to the above data, only one of the observed signals shows a similarity with a typical meteoroid entry signal, which can seen on the output of event detector for the actual date shown in Fig. 39.

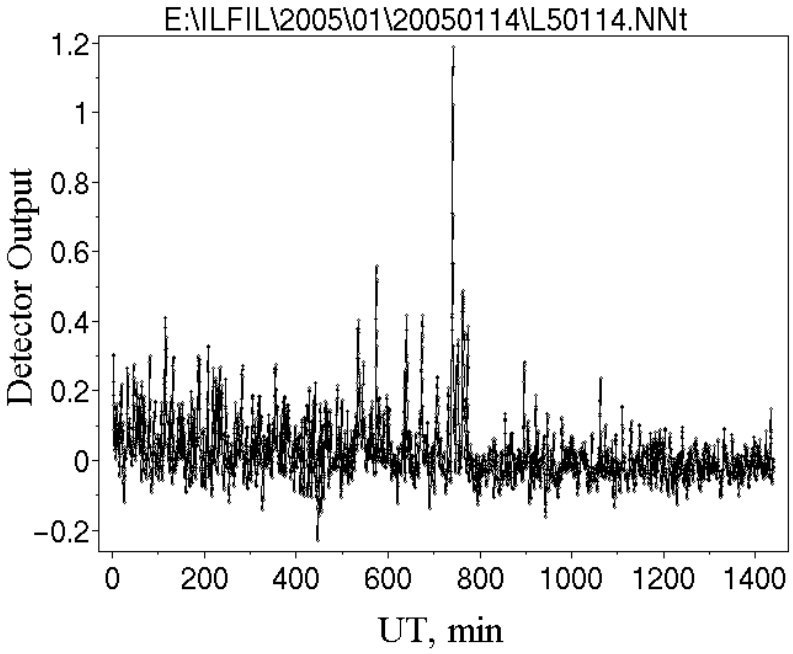

Fig. 40. An example of the event detector output for the same date as shown in Fig. 39.

The last step of the automatic data screening is to correlate the largest detector outputs (only those larger than 0.5) with validated signals (like those shown in Fig. 39).

Unfortunately, some other supersonic objects, like aircraft and rockets, may occasionally generate signals very similar to those produced by meteoroid entries. These signals will also produce large event-detector outputs. For this reason, the list of event-detector outputs was manually reviewed to investigate plausibility of the detection. The following criteria were used:

- A long-lasting infrasonic signal, which sometimes produces the detector indication, is most likely some other kind of supersonic object.
- For distant objects, a nearly constant trace velocity indicates a supersonic aircraft rather than a meteoroid entry.
- During the analyzed 10-year period, it is possible to check if possible entry events repeat at the same position of the Earth with respect to the Sun (day number).
- When the object's velocity can be measured (see a later section), additional information may be drawn about its nature.

Results of the Data Screening Procedure

Unfortunately, the data coverage and data quality were not as good before year 2000 as they are now, which must be remembered when interpreting the analysis results. The occurrence of all possible events (detector outputs connected with events with a plausible angle-of-arrival and trace velocity variations) is presented in Fig. 41. The results are presented in a bar-graph, especially suitable for the demonstration of recurrent events. Years are plotted along the y-axis and day numbers along the x-axis. For recurrent events, the bars, marking each individual event, are "melting" together, enhancing the colour of the bar.

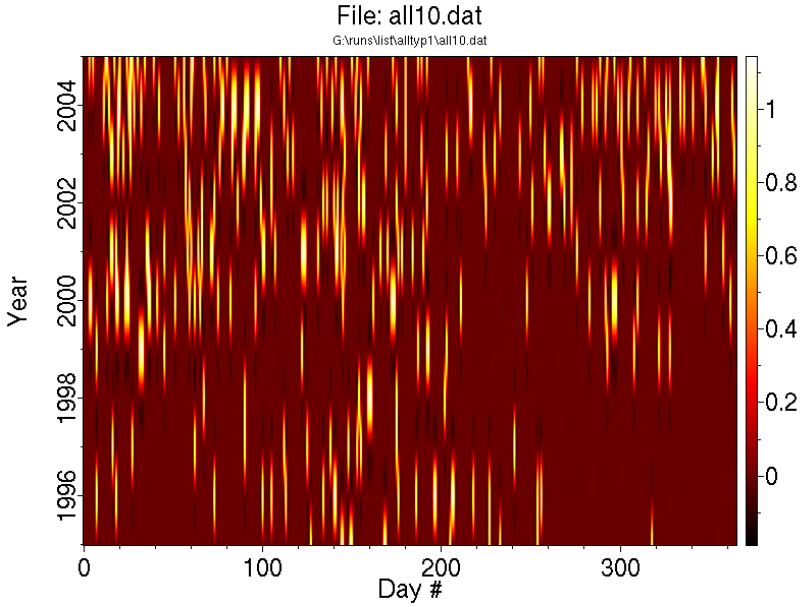

Fig. 41. Occurrence of all possible events as a function of the year and day number. The z-scale shows the weight calculated by the interpolation routine. The maximum weight = 1 is obtained when an event occurs at the same day number during at least two consecutive years.

The picture changes somewhat if only events occurring at least twice on the same day nr are accepted. The result is shown in Fig. 42.

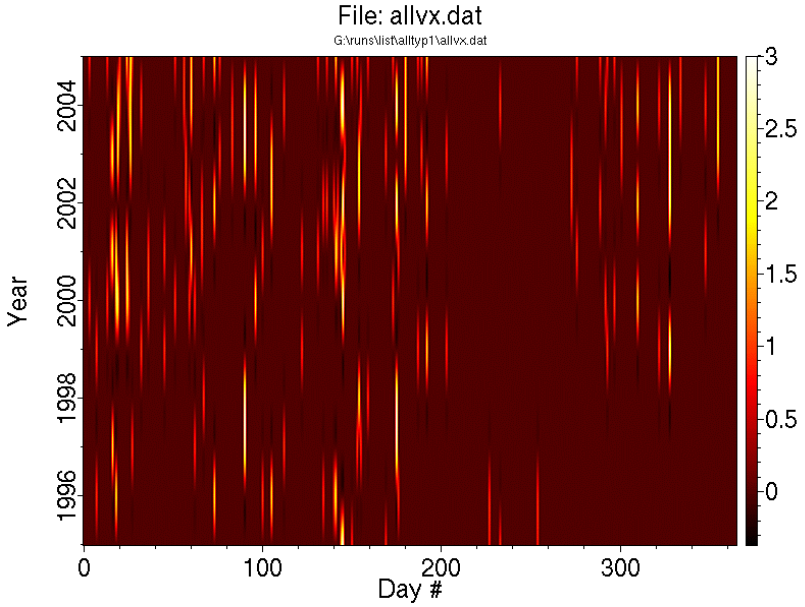

Fig. 42. Occurrence of those possible events, which repeats at least twice on the same day nr, as a function of the year and day number. The z-scale shows the weight calculated by the interpolation routine. The maximum weight is here n-1, where n is number of events at a given day number.

It is interesting that, when compared with optical observations of meteors (worldwide observations of magnitudes between –6 and –4), there is a complete lack of recurrent events during summer months, when there is a maximum of visual meteor events. This may indicate that events detected in the infrasound range, which if confirmed optically, correspond to events brighter than –10 mag, may belong to a different population than rather faint optical events.

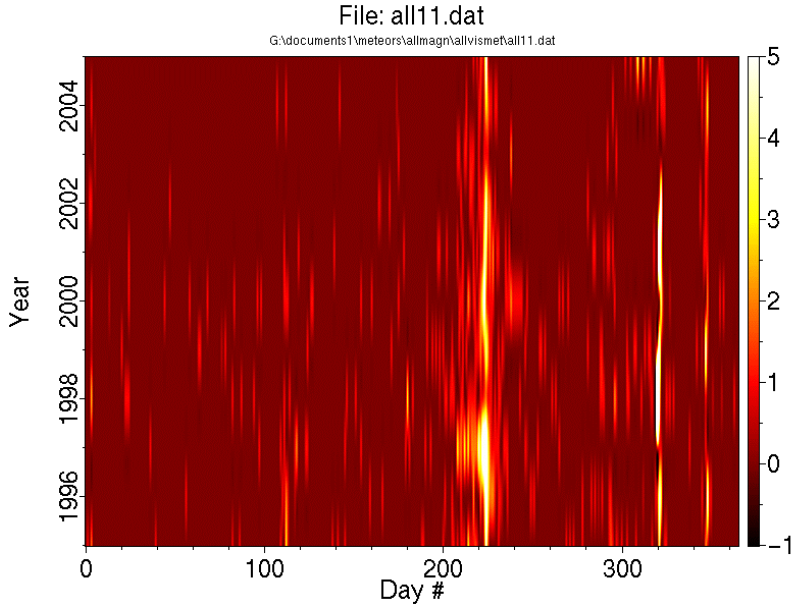

Fig. 43. Number of visual meteors (between –6 and –3 magnitude) per day. The graph is compiled using the data from International Meteor Organization tables at http://www.imo.net/data/visual. The z-axis indicates the number of events per day.

The total number of visual meteors, during 1995 – 2005, obtained through summation of data in Fig. 43 is shown in Fig.42.

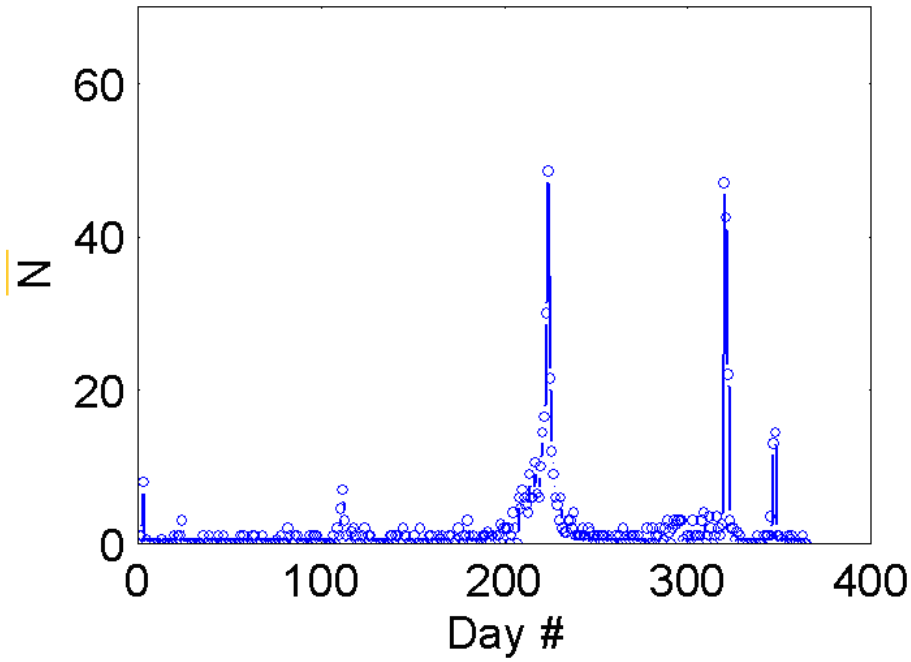

Fig. 44. Total number of meteors/day brighter than –3 mag during the period 1995-2005.

A similar graph has been constructed (Fig. 45, blue bars) adding up possible recurrent events presented in Fig. 42. On the same graph, visually observed major events are plotted (red bars).

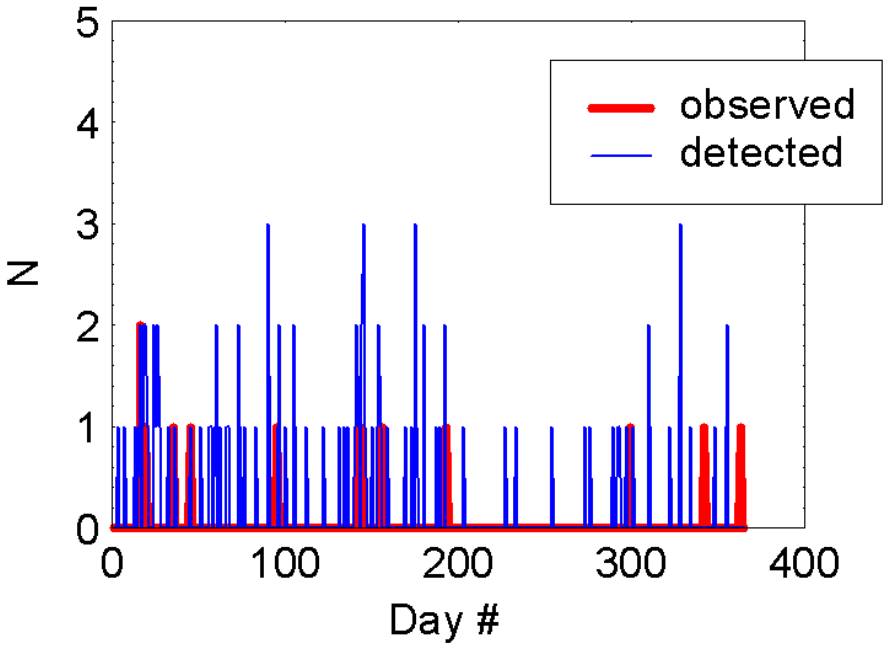

Fig. 45. A comparison between detected possible events (blue bars) with visually confirmed, and at the same time observed with infrasound, events (red bars).

Confirmed events, which were not used as the reference events, are listed in Table 3.

Table 3

Date	Location
1997-12-09	Greenland
2002-01-17	Netherlands
2002-02-15	Vemhån, Sweden
2002-06-06	Mediterranean
2002-12-30	Morjärv, Sweden
2004-05-23	Lycksele, Sweden

Some of above events were observed only locally in Sweden. Two of observed events are in particular interesting: 2002-01-17 in the Netherlands (see http://home.wanadoo.nl/marco.langbroek/17_01_02.htmle.woo.nl/marco.langbroek/17_01_02.html) and 2004-01-17 in Jokkmokk, northern Sweden. These are both major events, and the 2002-event was attributed to the delta Cancrid meteor shower occurring around January 17 each year. There are several detections of possible events on and around January 17 during the analyzed period 1995-2005. A remarkable observation was made on January 20, 2004. This event was most likely a meteoroid entry E of Greenland. The event was recorded at Kiruna, Lycksele and Uppsala at distances larger than 4,000 km, which indicates a considerable yield of the event. It was, however, smaller than 20 kton TNT, since it was not detected by the surveillance satellites (ReVelle, private communication).

All events for which heading could be determined are plotted in Fig. 46.

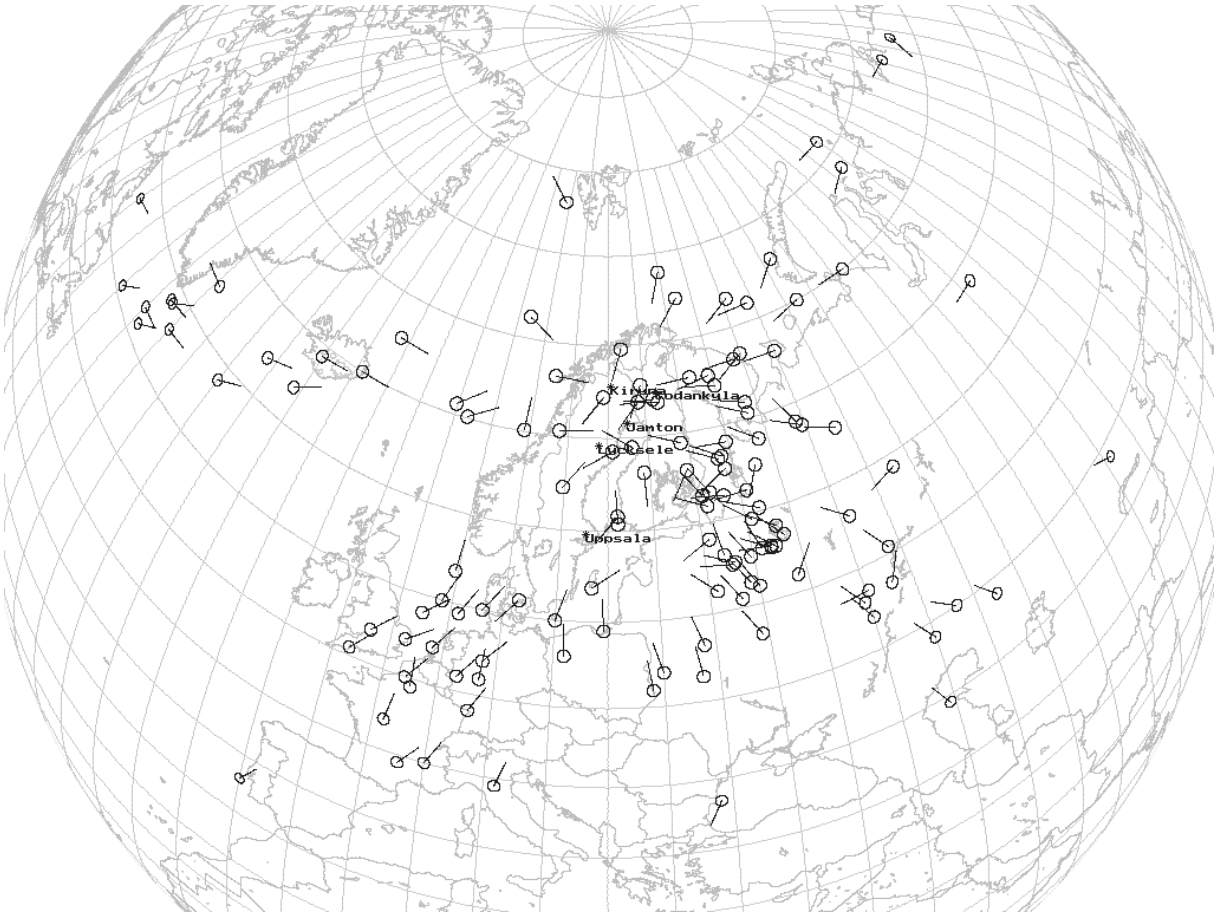

Fig. 46. Location of all events for which the heading was determined. Headings marked by line segments.

One must keep in mind that only objects having a non-zero velocity component in the direction towards an array can be detected. In order to localize an event, this condition must be fulfilled for at least two arrays.

Chapter 7

Detection of High Trace Velocity Events

Two minor meteor events, observed by only one station, were found to be associated with signals with very high horizontal trace velocities across the array (being a measure of the source elevation). In these cases, there is an indication that the sources were nearly overhead. Their spectral content (lack of high frequencies) also indicates a great source height.

Unexplained signals with very large amplitudes and high horizontal trace velocities were occasionally observed at SIN stations in the past. Many of these signals were earlier discarded, assuming being a result of local interferences. Here, a systematic search for these events is carried out.

Locally Observed Meteor Events

Most smaller meteor events, reported in local media, cannot be verified in the SIN's data, probably because of their range of detection. There were, however, two events, which took place close enough to a SIN array.

Morjärv event of December 30, 2002

On December 30, 2002, eyewitnesses reported a distant sonic boom, later followed by a swishing sound near the village of Morjärv in northern Sweden. Due to complete cloud cover in the region, there were no reports of an observed fireball. During the following day, a number of circular (10 – 20 cm) marks cleared of snow in the otherwise very even snow cover were found on the neighbouring lake. The sonic boom was confirmed by the Jämtön array, only 26 km SSW of the reported impact area. The infrasonic signal arrived from a direction of 208 degrees, which means that the explosion occurred more than 30 km from the impact area. The signal was distinct and of short duration, with a high cross-correlation between the microphones and high trace velocity, indicating that the source was very close.

The amplitude recording of the event is shown in Fig. 47.

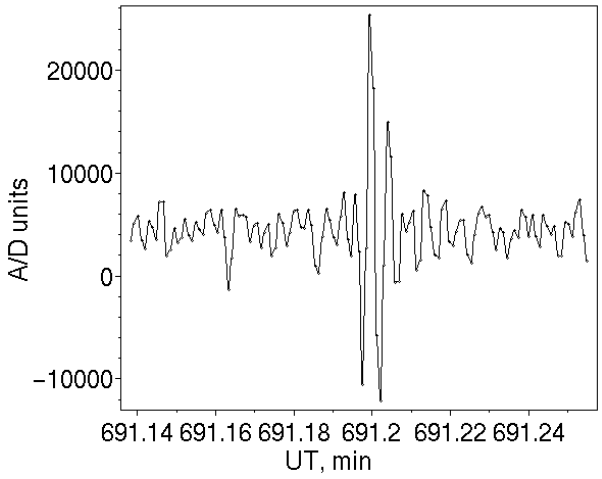

Fig. 47. Amplitude recording of the infrasonic signal from the Mörjärv-event

Lycksele event of May 23, 2004

On May 23, 2004, an event was reported to the media. Around noon, local time, people in villages NE of Lycksele heard a sound, like distant thunder. However, there was no thunderstorm activity on that day in the region and since it was a Sunday, a supersonic boom could be excluded. A few days later, villagers found a fresh 1.5 meter crater in a swamp, close to a small private road, see Fig. 48, approximately 25 km from the Lycksele-array. A search in the Lycksele-data from that day showed a signal (Fig. 49) at 1124UT with a very high trace velocity and the angle-of-arrival of 43 degrees, which is in perfect agreement with the location of the crater. Attempts were made to dig in the crater, however no debris was found. The swamp is 2.2 meters deep at the impact location.

Fig. 48. A 1.5 m crater in a swamp attributed to the Lycksele event.

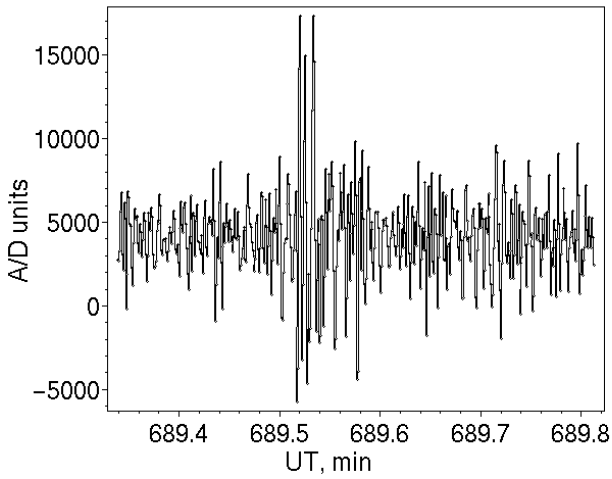

Fig. 49. Amplitude recording of the infrasonic signal from the Lycksele-event.

A Search for the High Trace Velocity Events (HTV)

An automated search was made for high trace velocity events (HTV) in the last 5 years of data. During the year 2000, the infrasonic stations were equipped with 16-bits A/D converters. In order to increase the reliability of possible findings, the search was limited to the period with higher accuracy of A/D conversion.

The search resulted in unexpected results: it appears that HTV signals are very common at Kiruna and Lycksele, but unusual at Jamtön and Uppsala. Up to hundreds of HTV signals per day may occur at Kiruna and Lycksele. A typical example of a HTV signal is shown in Fig. 50, together with its wavelet spectrum. The figure shows that the signal is nearly saw-tooth shaped, reach in harmonics. At its maximum, the first harmonics is clearly seen on the wavelet spectrum.

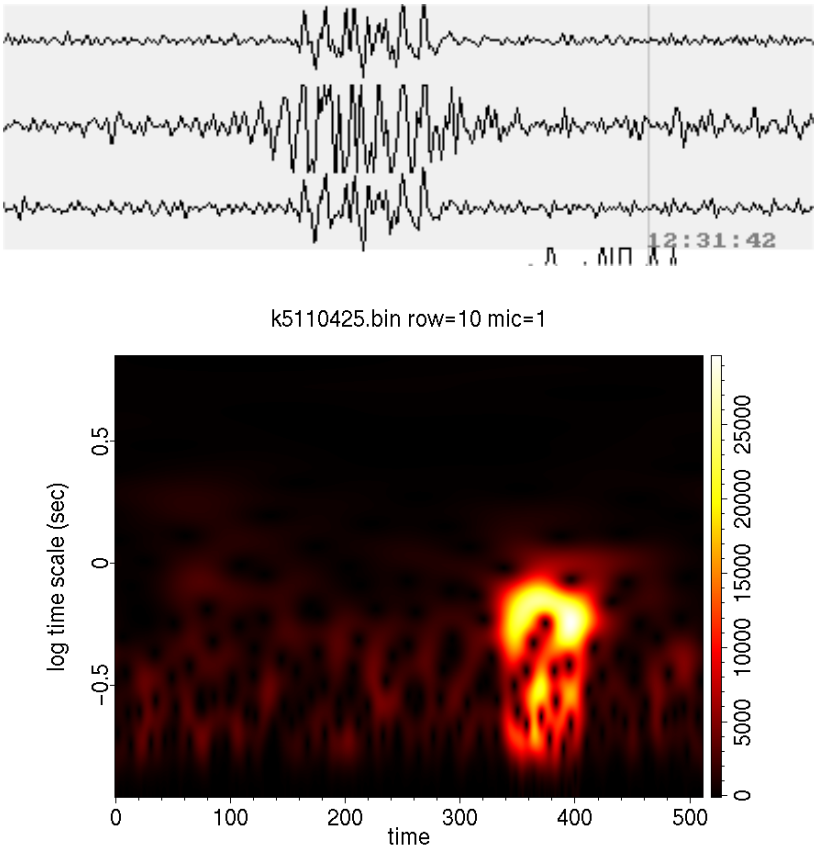

Fig. 50. A typical HTV signal (upper graph), recorded at 3 microphones at the Kiruna array. The lower graph shows the wavelet spectrum of the signal from Microphone 3. The time scale axis is logarithmic and the time axis is marked in sample nr:s, (18Hz sampling rate).

The HTV signals also have other unusual properties. The most surprising property is that they are nearly simultaneous at both stations, 365 km apart! This can be seen in the example of Fig. 51, showing the angle-of-arrival of three different HTV signals occurring on October 31, 2005 between 650 – 653 UT (10:50 – 10:53UT). Two of the signals are practically simultaneous at both arrays; the middle one starts 12 seconds earlier in Kiruna than in Lycksele.

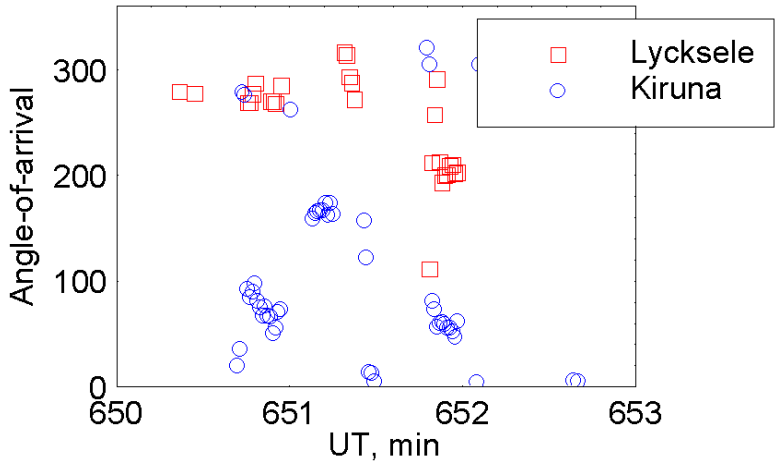

Fig. 51. Angle-of-arrival for three different HTV signals occurring between 650 – 653 UT (10_50 – 10:53UT) on October 31, 2005, recorded at Kiruna and Lycksele.

Corresponding trace velocities are shown in Fig. 52. Trace velocities vary during these three events between 1000 and 20000 m/sec (20 – 1 degree zenith distance of the wave normal).

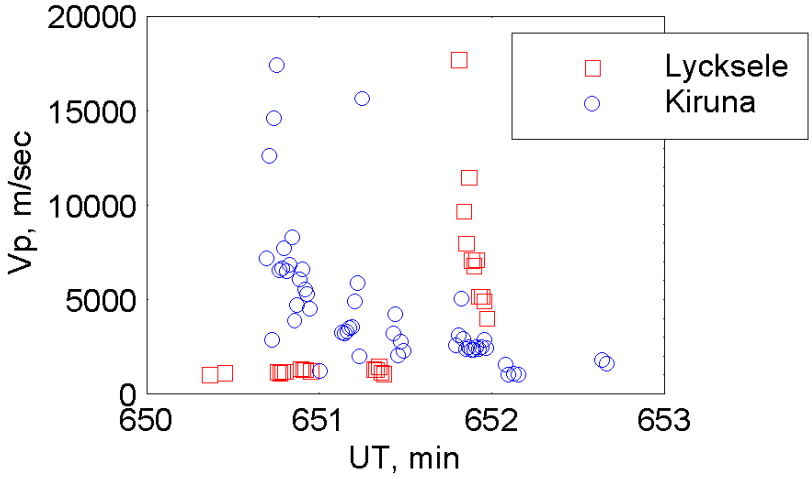

Fig. 52. Trace velocities during three events of Fig. 51.

Since the wave arrives practically from the zenith, it is not meaningful to draw any conclusions from the measured angle-of-arrival.

Properties of the observed HTV signals do not fit into present knowledge about known infrasound sources. Some of these signals may be attributed to small, overhead, meteor events, but certainly not those occurring nearly simultaneously over a 365 km distance. The signals cannot be connected to auroral activity, since they are most common during daytime, far from the auroral oval. The cases shown in Figs. 51 – 52 occur during a perfectly magnetically quiet period, so they cannot be due to magnetic disturbances.

There is one possible explanation for HTV signals. On October 31, 2005, in the late morning, a front passed across northern Sweden. A possibility of the forming of acoustic solitary vortices in the vicinity of temperature gradients has been discussed during the past 20 years (Stenflo, 1987). HTV signals could be low frequency emissions generated by such solitary vortices, solitons, distributed along the front. What was assumed to be a simultaneous

occurrence at two distant places could be purely accidental. Further experiments are needed to confirm the nature of HTV signals.

Reference to Chapter 7

Stenflo, L.: Acoustic solitary vortices. Phys. Fluids, 30 (10), 3297, 1987.

Concluding Remarks

It has been shown that a network of infrasonic arrays may be used as an efficient tool for the detection of meteoroid entries. The events may be detected and localized at distances on the order of several hundreds of kilometres. At close distances, below 100 km, the measured horizontal trace velocity may be used as a measure of the apparent elevation of the source. In this case, also orbital information about the meteoroid can be obtained. This means that the spacing of arrays in the present SIN is too large in order to efficiently determine orbital elements of meteoroids entering the Scandinavian region.

An advantage of the infrasonic observations is their low cost. A simple 3-microphone array, a data acquisition unit with software and access to Internet are needed for automatic monitoring of infrasound. A network of arrays separated by distances of about 100 km would provide an excellent regional coverage of all detectable meteoroid events.

About the Author

Ludwik Liszka graduated in Physics and Astronomy from the Jagiellonian University, Krakow, Poland in 1957. In 1958 he started his career as a scientist at the Kiruna Geophysical Observatory in Sweden (presently the Swedish Institute of Space Physics, IRF). In 1963 he received a PhD in Physics from Stockholm University, Sweden for a thesis in the area of Ionospheric Physics. In 1975 he was appointed as Associate Professor and Head of the Technical Division of the National Board for Occupational Health in Umeå, Sweden where he studied the effects of noise and vibration on humans. The same year he was awarded the Wallmark Prize by the Royal Swedish Academy of Sciences for his work on the long-distance propagation of infrasound from man-made sources. In 1983 he was appointed as Professor at the Swedish Institute of Space Physics where his special interest was in the area of application of artificial intelligence methods in space-science and technology. His other areas of interest are studies of long-distance propagation of infrasound and applications to detect remote events. He is the author of numerous scientific publications in the areas of ionospheric- and space physics, infrasound propagation, solar physics and astrophysics.

Ludwik Liszka is a Member of the Royal Swedish Academy of Engineering Sciences.

Institutet för rymdfysik

Swedish Institute of Space Physics

Swedish Institute of Space Physics
Box 812, SE- 981 28 Kiruna, SWEDEN
tel. +46-980-790 00, fax +46-980-790 50, e-post: irf@irf.se

www.irf.se